Development of Data Acquisition and Control System for Transfemoral Prosthesis Testing Platform

Author

Afnan Ahmed Yaqub

Regn Number

00000205287

Supervisor

Dr. Mohsin Islam Tiwana

DEPARTMENT OF MECHATRONICS ENGINEERING

COLLEGE OF ELECTRICAL & MECHANICAL ENGINEERING

NATIONAL UNIVERSITY OF SCIENCES AND TECHNOLOGY

ISLAMABAD

AUGUST, 2021

This page is intentionally left blank.

Development of Data Acquisition and Control System for Transfemoral Prosthesis Testing Platform

Author

Afnan Ahmed Yaqub

Regn Number

00000205287

A thesis submitted in partial fulfillment of the requirements for the degree of

MS Mechatronics Engineering

Thesis Supervisor:

Dr. Mohsin Islam Tiwana

Thesis Supervisor's Signature: _____

DEPARTMENT OF MECHATRONICS ENGINEERING

COLLEGE OF ELECTRICAL & MECHANICAL ENGINEERING

NATIONAL UNIVERSITY OF SCIENCES AND TECHNOLOGY, ISLAMABAD

AUGUST, 2021

Declaration

I certify that this research work titled "*Development of Data Acquisition and Control System for Transfemoral Prosthesis Testing Platform"* is my own work. The work has not been presented elsewhere for assessment. The material that has been used from other sources it has been properly acknowledged / referred.

Signature of Student

Afnan Ahmed Yaqub

00000205287

Language Correctness Certificate

This thesis has been read by an English expert and is free of typing, syntax, semantic, grammatical and spelling mistakes. Thesis is also according to the format given by the university.

Signature of Student

Afnan Ahmed Yaqub

Registration Number

00000205287

Signature of Supervisor

Dr. Mohsin Islam Tiwana

Copyright Statement

- Copyright in text of this thesis rests with the student author. Copies (by any process) either in full, or of extracts, may be made only in accordance with instructions given by the author and lodged in the Library of NUST College of E&ME. Details may be obtained by the Librarian. This page must form part of any such copies made. Further copies (by any process) may not be made without the permission (in writing) of the author.
- The ownership of any intellectual property rights which may be described in this thesis is vested in NUST College of E&ME, subject to any prior agreement to the contrary, and may not be made available for use by third parties without the written permission of the College of E&ME, which will prescribe the terms and conditions of any such agreement.
- Further information on the conditions under which disclosures and exploitation may take place is available from the Library of NUST College of E&ME, Rawalpindi.

Acknowledgements

All praises for the Almighty creator Allah Subhanahu-Wata'ala and salutations for His Last Messenger Muhammad (S.A.W). None of this work could be realized without Allah's blessings in every aspect including knowledge, health, and the ability to observe, investigate, infer, create, and implement.

I am particularly thankful to my beloved parents whose continuous efforts and sacrifices have excelled me towards this accomplishment in my life. My gratitude to my wife and kids for their patience.

My utmost respect and thanks to my supervisor Dr. Mohsin Islam Tiwana for his trust in me and my ability and also for his timely guidance when I was facing challenges in the completion of my project.

Finally, I would like to express my gratitude to all the individuals especially Mr. Muhammad Zawar ul Hassan and Mr. Rizwan Ullah Khan who have rendered valuable assistance to my study.

Dedicated to my exceptional parents, my wife and kids and the rest of my family who have always provided tremendous support and cooperation that led me to this wonderful accomplishment

Abstract

A data acquisition and control system for a 2 DOF platform for testing of transfemoral prosthesis is developed. The system is based on a PC with an attached motion control setup where target position trajectories are loaded for both the human hip vertical motion and the thigh angular motion. A servo motor is actuated to move a carriage in vertical axis tracking the motion profile of a human hip. Another servo motor attached to the carriage is actuated to exhibit the angular motion profile of a thigh. A prosthetic limb can be attached to the carriage. Upon simultaneous actuation of the two servo motors the prosthetic limb can be moved exhibiting the gait cycle of a human leg.

Key Words: *2 DOF, transfemoral, prosthesis, gait, testing, control, motion profile, tracking, servo motor*

.

Table of Contents

List of Figures

List of Tables

CHAPTER 1: INTRODUCTION

1.1 Research Motivation

Amputee rehabilitation is a slow process often requiring huge effort from the patient and rehabilitation treatment team. Involving patients in research and development and testing of a prosthesis product, also known as in-vivo testing, is not feasible as it is a tiresome activity for the patient. It also does not support the requirement of performing cyclic testing and acquiring repeatable results from such tests. Testing such products without involving patients, called in-vitro testing, is the solution. A testing platform is therefore most suitable option for running cyclic tests for prosthesis products. Rugged platforms designed for running hundreds of thousands of cycles for testing prosthesis products can be manufactured and employed. Tracking typical or specific human gait target trajectories is possible for cyclic testing of prosthesis and performing load and stress testing activities.

A robotic platform has been developed by Department of Mechatronics Engineering at the College of Electrical and Mechanical Engineering, National University of Sciences and Technology. A transfemoral prosthesis can be mounted on a carriage attached to the platform. The platform has been designed to allow the vertical hip motion and the angular motion of the thigh so that the prosthesis can be moved according to human gait profile. The function of the platform is to perform cyclic testing of the attached transfemoral prosthesis. The system can also be used to test unstructured events such as simulating a walk on an irregular terrain and observing the effects on the prosthesis.

1.2 Statement of Problem

The problem is to make a prosthetic leg move in a manner of human leg. This is required for the cyclic testing of the prosthesis to ensure its proper functioning for the desired number of cycles equivalent to the activity of a human leg. This must be done by simultaneous motion of the hip and thigh motors in accordance with their respective motion profiles. Error in execution of the motion trajectories will result in inadequate performance of the system and may cause damage.

1.3 Thesis Contribution

This thesis is intended to explain the design development and deployment of the control setup for the transfemoral prosthesis testing platform. The controller is implemented for controlling the actuation of two AC servo motors installed on the robotic platform so that the attached prosthesis can execute the profile of human gait in sagittal plane. One of these motors upon actuation moves the carriage in the vertical axis thereby imparting the hip profile movement to the attached prosthesis. The second motor is attached to the carriage and upon actuation allows the prosthesis to execute the profile of the human thigh. Both these movements are in the sagittal plane. The two motors are to be actuated together thereby allowing the prosthesis to execute a motion profile like human leg in the sagittal plane.

1.4 Project Impact

This project provides a basic control platform for research in the field of biomechanics. Although the system has been developed with the aim of performing cyclic testing of lower limb prosthesis, yet the system can be effectively utilized in understanding and developing control techniques for humanoid robot mobility.

The system can be used in performing research on motion control of individual limbs while simulating terrestrial locomotion scenarios such as motion on inclined paths or irregular terrains. It may also allow the study of motion control scenarios in various kinds of unstructured situations that may challenge a pedal locomotion.

With the ever-increasing interest in the area of artificial intelligence and machine learning, the system can be a very useful platform for studies of motion control using neural networks.

1.5 Thesis Breakdown

The following chapters discuss the various steps involved in the design and development of the control scheme for the transfemoral prosthesis testing platform. Chapter 2 explains the literature review. Chapter 3 discusses the methodology adopted for the control. The hardware software and control scheme are detailed herein. Chapter 4 details the results and discusses the outcomes of the project. Finally, in Chapter 5 the conclusion and future work is provided.

CHAPTER 2: LITERATURE REVIEW

2.1 Human Anatomy and Gait

Anatomy is a Greek word meaning ‘dissection’ or ‘to dissect’. A comprehensive explanation of human anatomy is given at [1]. It is the study of structure of human body. The study of human body involves step by step learning the terminology for various parts, their locations, body planes also known as anatomical planes, movements, and directions. The study of anatomy is broadly categorized into two categories

a. Macroscopic or gross anatomy
b. Microscopic anatomy.

2.1.1 Macroscopic Anatomy and Lower Limb

The location of major components of human body structure or its topography is studied in macroscopic anatomy. The macroscopic or gross anatomy is studied with two fundamental approaches i.e., a regional approach and a systemic approach. The regional anatomy organizes the body into head and neck, the trunk, upper and lower limbs. The human locomotion is achieved by the movement of lower limbs.

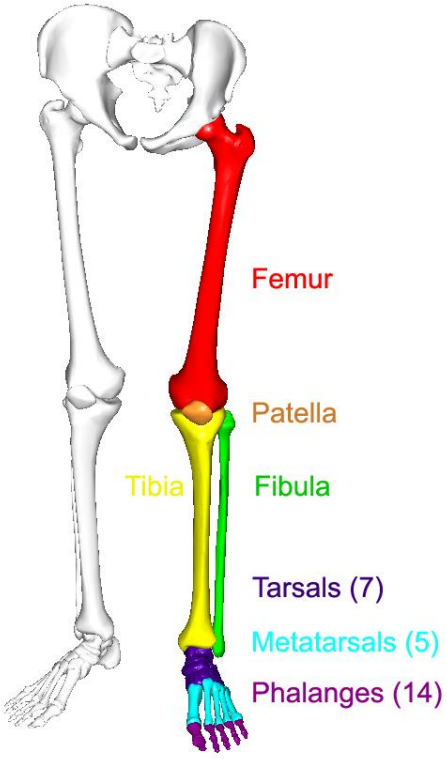

Figure 1 Parts of the lower limb [2]

The lower limb is composed of hip, thigh, leg, and foot. The mobility is dependent on the flexibility of hip, knee, and ankle joints. The thigh is composed of single bone called Femur. The leg has two bones i.e., tibia and fibula.

2.1.2 Anatomical Planes

The positions and relations of various anatomical structures in human body are studied in various planar views. The reference planes for these views are three anatomical planes. [3] explains anatomical planes in detail. These are the coronal or frontal plane, the sagittal or lateral plane and the transverse or axial plane. Although the human cadaveric gait is a complex 3-dimensional movement, the forward propulsion of the body is executed and therefore mainly analysed in the sagittal plane.

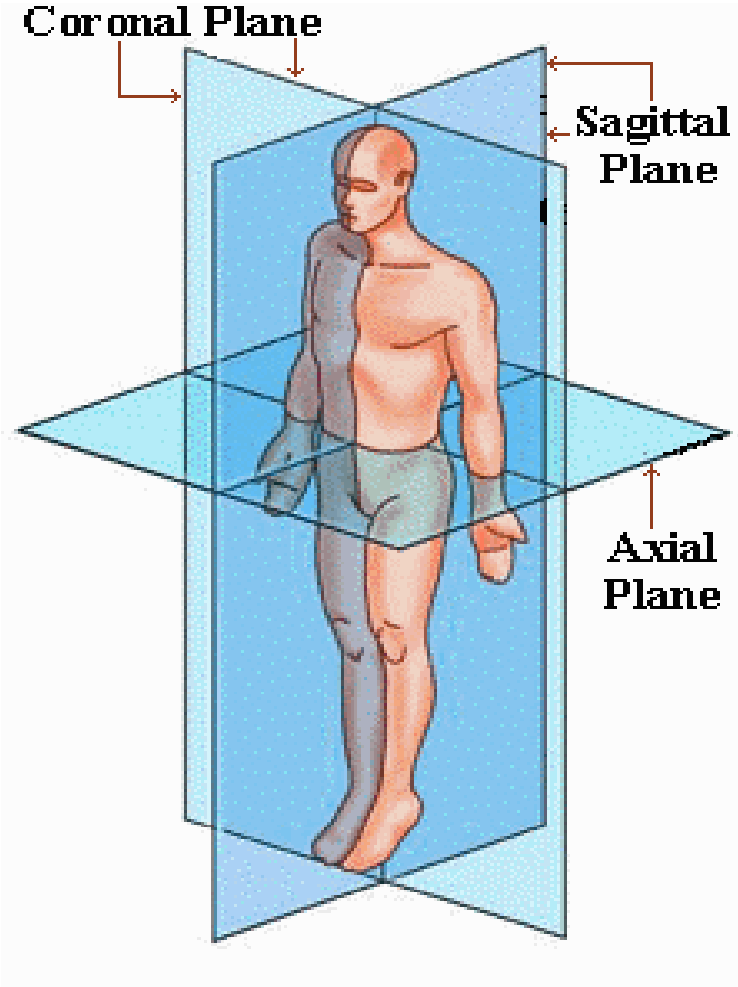

Figure 2 Anatomical planes [3]

2.1.3 Human Gait

Human gait is the forward propulsion of human body in the sagittal plane. The profiles that human leg executes during a normal walk analysed in the sagittal plane has been the prime topic of the literature review. Human gait is a bipedal motion executed in two phases. The first phase is called the Stance Phase and is characterized by striking of heel of one foot on the ground till the toe off for the same foot.

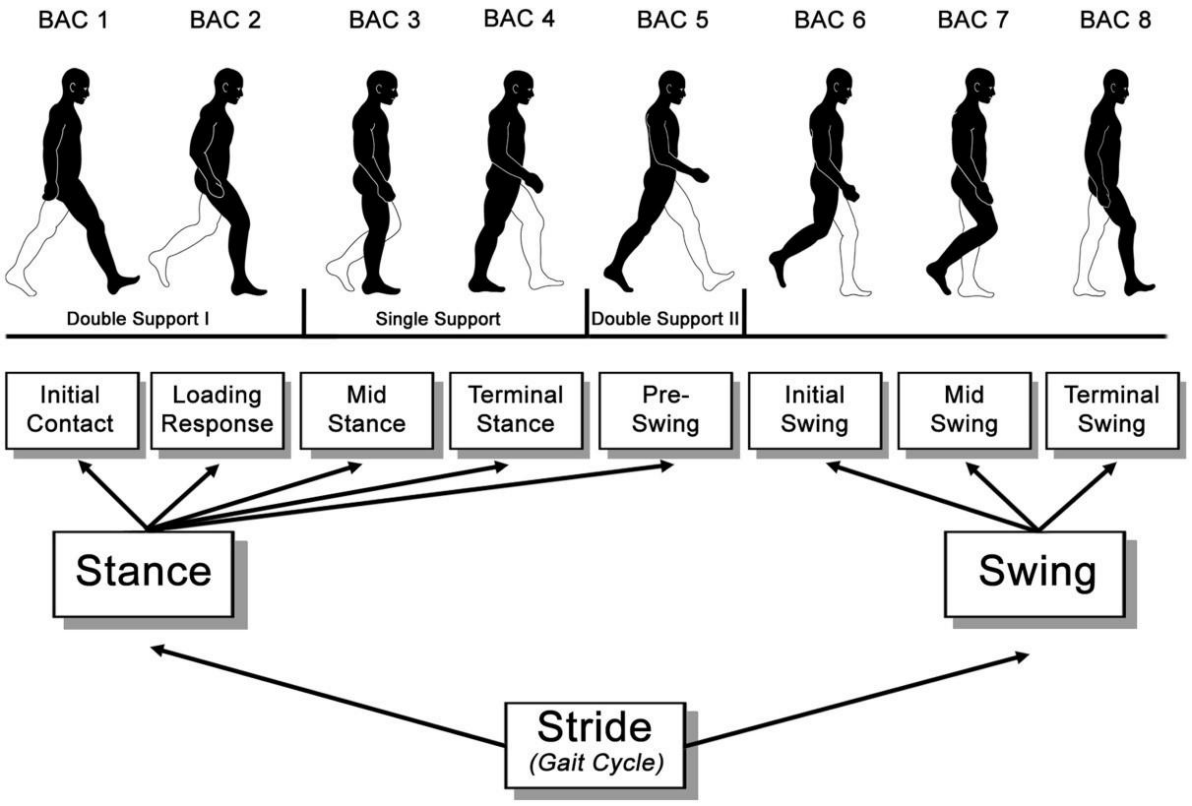

Figure 3 Functional Divisions of a gait cycle [4]

The stance is divided into five sub-phases i.e., initial contact, loading response, mid stance, terminal stance, and pre-swing. This completes 60% of the gait cycle. The second phase called the Swing Phase is from the toe off till the next heel strike. The swing phase comprises three sub-phases i.e., initial swing, mid swing, and terminal swing. This completes the remaining 40% of the gait cycle. During stance phase the other foot is in swing phase. A complete gait cycle thus comprises of two steps one by the alternate feet.

The name given to gait cycle is called a Stride. Figure 3 shows the functional divisions of the gait cycle as given by [4].

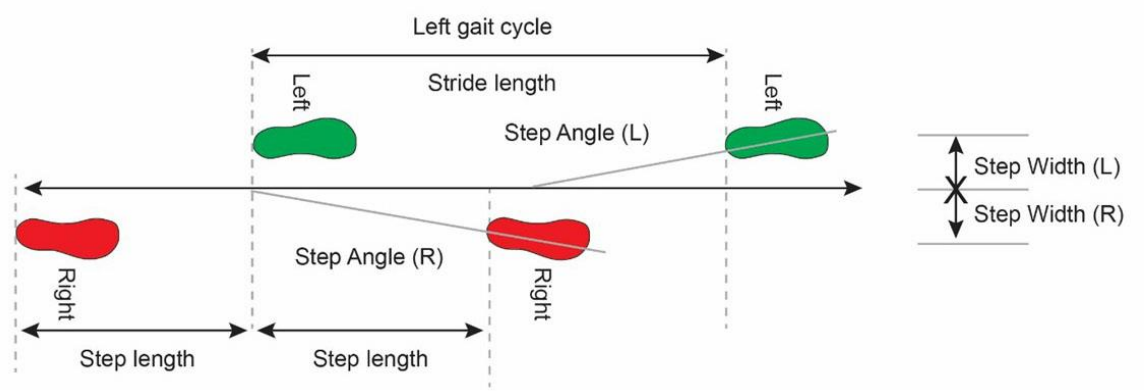

Figure 4 Gait Cycle of right and left feet [5]

2.1.4 Coordinate System

To study motion a reference coordinate system is necessary. A set of coordinate axes is attached to every part of the limb to understand its motion trajectory. For this study the reference system provided by [6]. A pictorial depiction is given in [7].

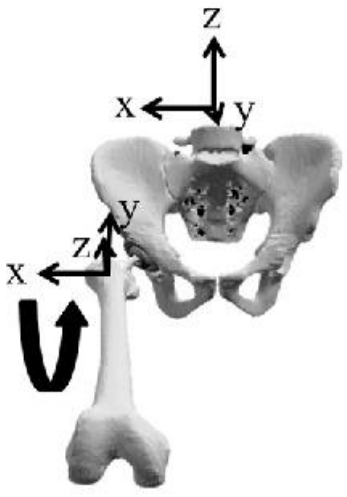

Figure 5 Coordinate system for pelvis and thigh [7]

2.1.5 Gait Data Set

Extensive data for human gait has been collected and analysed. A collection of gait data from [8] contains 1.5 hours of normal walk which amounts to more than 5000 gait cycles. It also contains 6 hours of perturbed walk which is more than 20,000 hours of gait data. This gait data has been collected from 15 subjects. The data includes gait events, 2-D joint angles, angular velocities and torques.

A subset of gait data collected from [4] is used in this project. This data is gathered from a software program known as human body model (HBM) with 44 degrees of freedom. It incorporates kinematics and kinetics computations in real time for muscle length changes and forces. The system has been used for gait analysis of 12 able-bodied individuals. This thesis utilizes the mean data for hip vertical motion and right hip flexion also available in the same data set.

2.2 Transfemoral Amputation

A surgical procedure performed to remove the lower limb at, or above knee is known as transfemoral amputation. A graphic depiction of various types of amputations on lower limb as given by [9] are shown below.

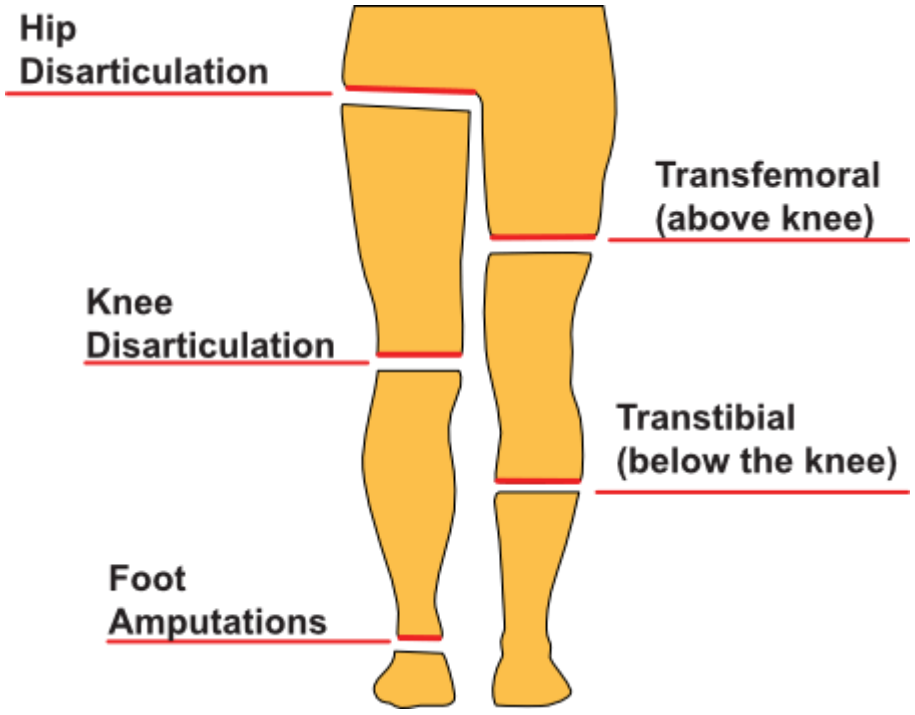

Figure 6 Types of lower limb amputation [9]

2.3 Transfemoral Prosthesis

A prosthesis is a device designed to replicate the functionality of a limb or a part of a limb. A transfemoral prosthesis is a device attached to the region between the hip joint and the knee joint. This thesis is about the control of a test platform for transfemoral prosthesis.

The socket of transfemoral prosthesis is attached to the residual portion of the leg of the amputee. Prosthesis of various types have been developed across the world. These include passive, semi-active and active. Figure 2 depicts the various parts of a transfemoral prosthesis.

Figure 7 Parts of a typical transfemoral prosthesis [10]

Most of the existing transfemoral prosthesis are of passive type [11]. However, a variety of prosthesis have been designed and developed because of extensive research in the field. From fully passive such as Mauch Knee (Mauch, 1968) to top of the line microcontroller-based prosthesis such as Otto Bock Genium exist and have been tested extensively. Efforts in this direction continue to provide the better product for the amputee so that mobility as closed to normal as possible can be provided.

2.4 Prosthesis Testing

Two approaches of testing prosthesis have been practiced. In-vivo testing involves testing and evaluating the prosthesis with the physical involvement of patient. This method is often problematic for the patient as it requires a lot of exhaustive effort by the patient. This approach also bars the possibility of performing cyclic testing as similar motion cannot be produced repeatedly.

The second approach is the In-vitro testing in which the limb is tested on a test bench without the involvement of the patient. This requires a complete system which can produce the complete motion of the human lower limb. Such systems have been previously developed by different research groups.

Different test benches have been developed for testing various types of lower limb prosthesis. [12] details the development of test bench for lower limb prosthesis with 40 degrees swing of femur and 40 degrees for tibia with respect to femur. Hip loading is provided by hydraulic actuator while walking is simulated by a motor driven sled that moves the foot.

Multi-component test bench has been developed by Department of Industrial Engineering, University of Padova [13]. With the help of two actuators, static and dynamic loading is provided on a running specific prosthetic foot while in contact with a surrogate ground inclined at different angles.

2.5 Control

The control of the system in this project requires understanding of the different strategies and types of controller implementations. After review of control literature the most appropriate and simple method is selected. An overview of the control literature follows.

2.5.1 Control Variables

Two of the most important signals in industrial control as stated by [14] are,

a. Process variable (PV)

b. Manipulating variable (MV)

The controller input is the process variable or PV. PV is measured by the sensors and fed to the controller. This is the variable that provides the decision basis for the controller.

The manipulating variable or MV is the variable that is interpreted in terms of controller output. For example, the voltage of the controller to control the speed of the motor.

2.5.2 Control Strategies

[14] lists the control strategies employed in the industrial control setups. These are,

a. On-Off Control

b. Open-Loop Control

c. Feed-Forward Control

d. Closed-Loop Control

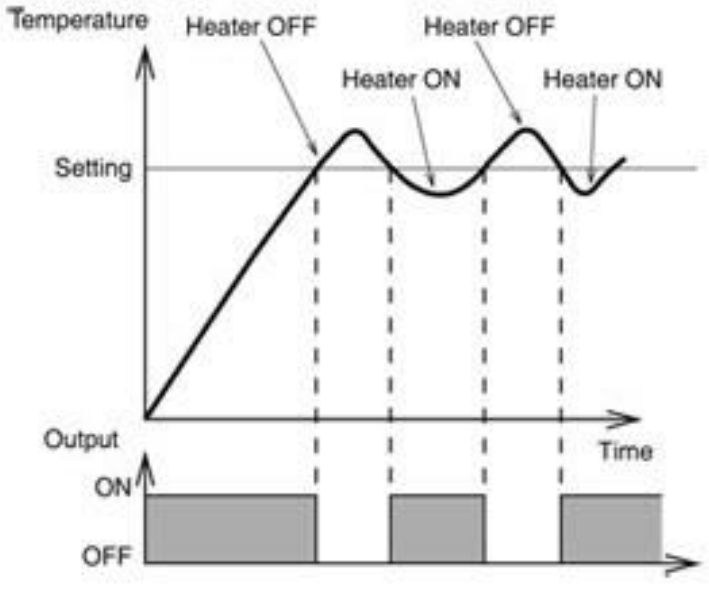

Figure 8 On-Off Control [14]

The On-Off control is the oldest control strategy used in systems where there are only two output states i.e., the system is either On or Off. The control turns the output to On state when the PV or measurement is below or above the set point or a given range. When the process variable is within the range or at the set value the controller turns the output Off. The On-Off control has oscillations and is prone to disturbances. It exhibits jittering on the output device. The solution is to add hysteresis between the On and Off sequences.

Figure 9 Open-loop Control [14]

The Open-Loop control is another simple form of control and does not monitor the process variable. The controller never knows the response of the system against the manipulating variable. This type of controller is best for situations where the disturbances in the environment do not exist.

Feed-Forward control is implemented to compensate for the disturbances in the system. The controller monitors the disturbances and adjusts the manipulating variable output to keep the system stable. This technique has complexities and require a better understanding of the overall process. Thus, expensive in implementation.

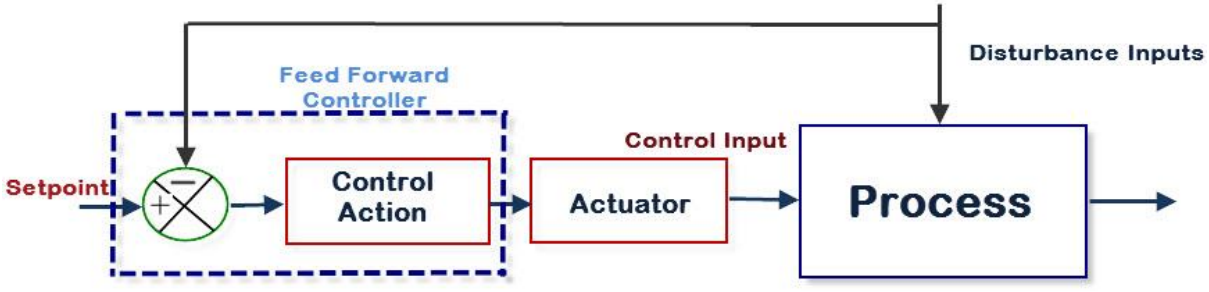

Figure 10 Feed-Forward Control [14]

Closed-Loop control is widely implemented in industry and the most reliable of all the strategies. In this strategy the controller continuously compares the measurement of output response with the desired value of the process variable. The difference is called the error. The controller adjusts the output accordingly to compensate the error in the system response.

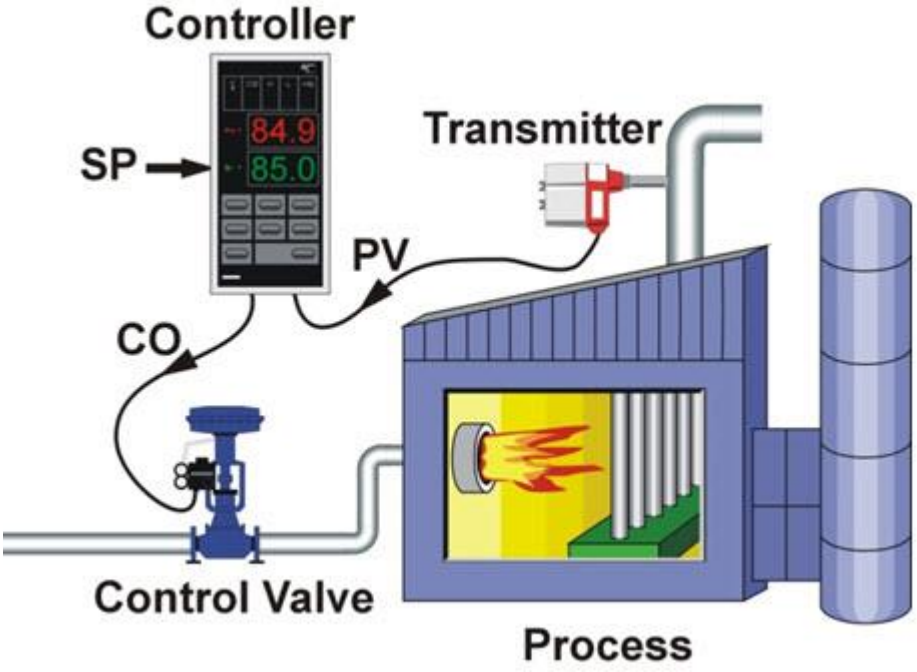

Figure 11 Closed-Loop Control [14]

2.5.3 Controller Types

In this project the configuration of the system matches a 2 degree of freedom (2 DOF) robot with one prismatic and one revolute joint. The motion is to be executed in the vertical plane. The control technique is therefore adopted after studying the literature associated to control of 2 DOF robotic platform in vertical plane.

The vertical plane robots exhibit a permanent tracking error due to the gravitational force vector. Tihomir et al., provides a comparative study of control algorithms for both the vertical and horizontal plane robot configurations. In this study the experimental evaluations have been done on the SCARA which is a 2 DOF robot manipulator in horizontal plane. The vertical configuration robot used for experiments is PELICAN.

[15] compares the following control techniques for closed loop controllers.

a. PD Controller
b. PID Controller
c. Fuzzy PID Controller
d. Classical Adaptive Controller
e. Neural Network Adaptive Controller
f. Analytical Fuzzy Controller

2.5.4 PD Controller

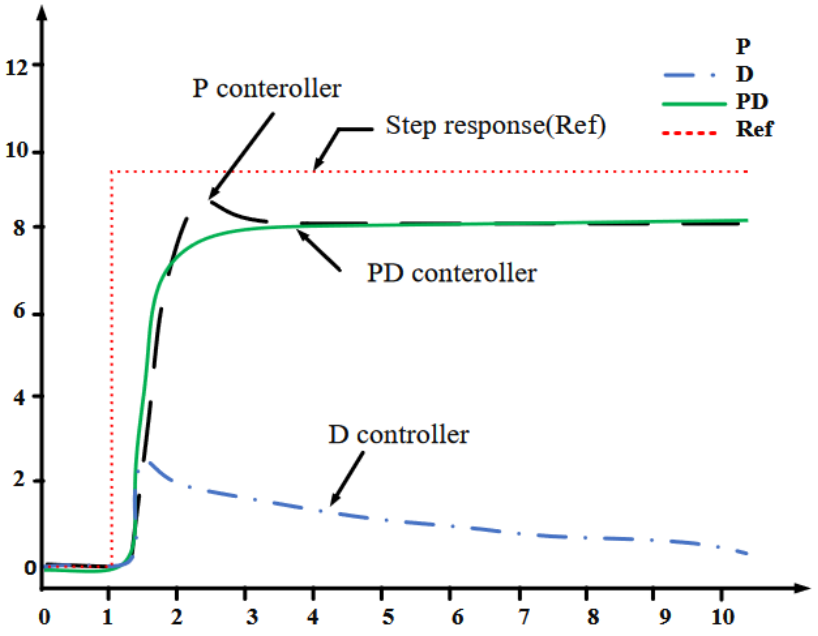

Figure 12 PD Controller Response Curves [16]

PD refers to the controller which compensates for the error in the plant output by adjusting a combination of proportional and differential gain in the output value against the current error.

The proportional component tries to minimize the error by directly influencing the output. Greater the error faster the change in output. The proportional gain is therefore adjusted in such a way as to minimize the rise time of the output value against a step change in input. This is known as the step response. However, greater the proportional gain, greater the off shoot.

The differential gain term works on the rate of change of error. As the error difference reduces so does the effect of the differential component. The overall change in output minimizes with the differential term.

PD controller is the simplest closed loop controller from implementation and stability point of view [15]. For horizontal plane robots PD controller provides asymptotic stability. However, PD controller is unable to compensate a permanent tracking error that exists for robots in vertical plane. Integral component must be added to remove the permanent tracking error for vertical plane robots.

2.5.5 PID Controller

PID is referred to the proportional, integral, differential control technique that calculates the output of the controller based on the current error in the plant output. In addition to the proportional differential term, it also contains an integral term. A typical representation is given below.

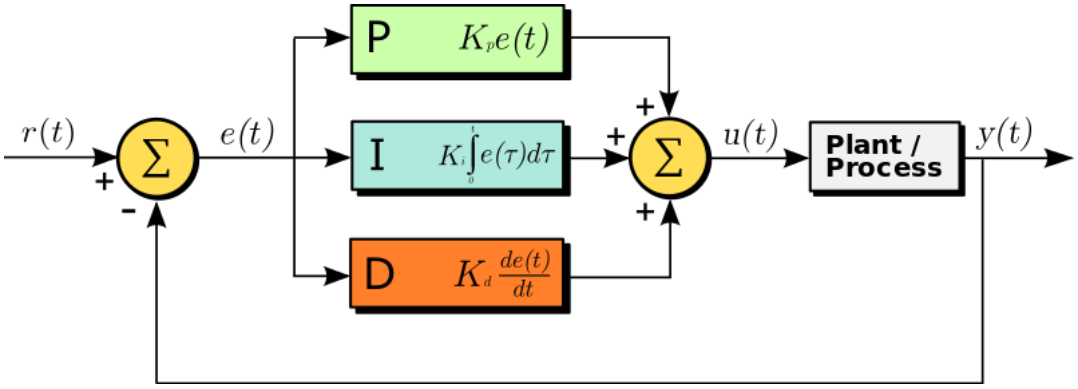

Figure 13 Typical Controller Diagram [17]

There exists, in a system, an error such that the response to the step input stays at a certain offset from the desired set point. This is known as the steady state error. The steady state error is removed by adjusting the integral gain of the system. The integral gain acts on the sum of error since the system received its step input. However, while the average error of the system approaches zero, the inclusion of integral error term introduces oscillations in the system about the set value. The integral term keeps track of the past errors and tends to remove the offset between the plant output and the set value.

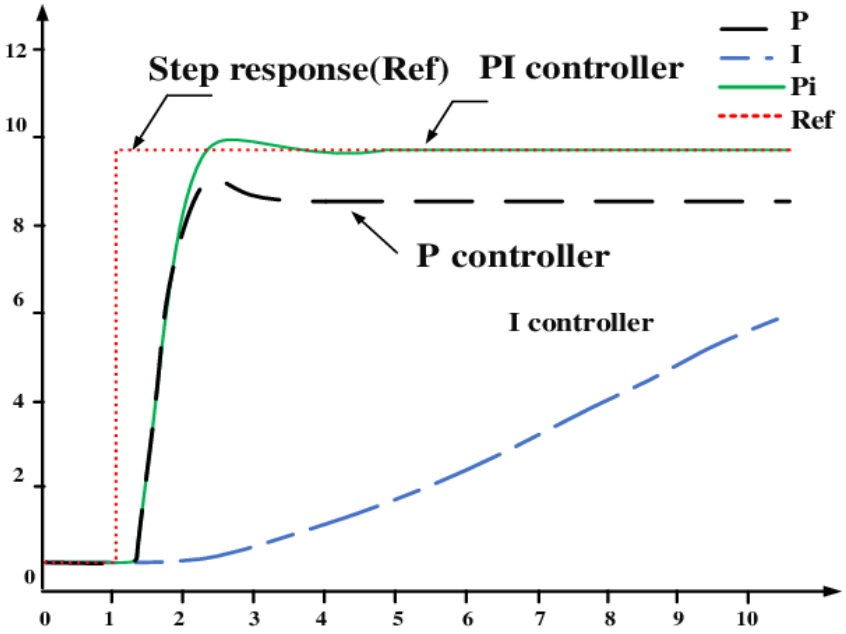

Figure 14 Integral Gain Response Curve [16]

The PID controller is also simple as far as the implementation is concerned. However, the stability analysis is complex in comparison with the PD controller.

2.5.6 Classical Adaptive Controller

The tracking of time variable position reference trajectory is efficiently carried out by classical adaptive controller. The implementation of classical adaptive controller is complex as its stability criteria is derived from the Lyapunov stability criterion which requires knowledge of regression matrix which drastically increases the computational cost as the system degrees of freedom increase beyond 2. For example, a 6 degree of freedom manipulator requires 425 multiplication and 369 addition operations. The implementation of this controller is computationally most demanding.

[18] has discusses two main types of adaptive control techniques. These are model reference adaptive control (MRAC) and self-tuning adaptive control (STAC) which have been used in recent research. In MRAC the system estimates parameters in order to behave similar to the reference model. In STAC the parameters are self-tuned to achieve an objective function such as minimization of error or maximization of efficiency.

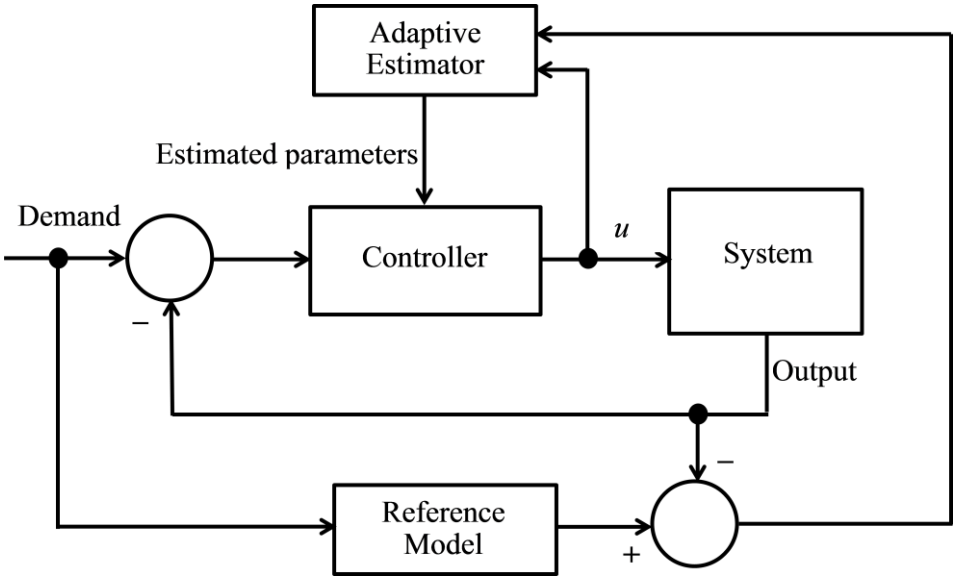

Figure 15 Model Reference Adaptive Control [18]

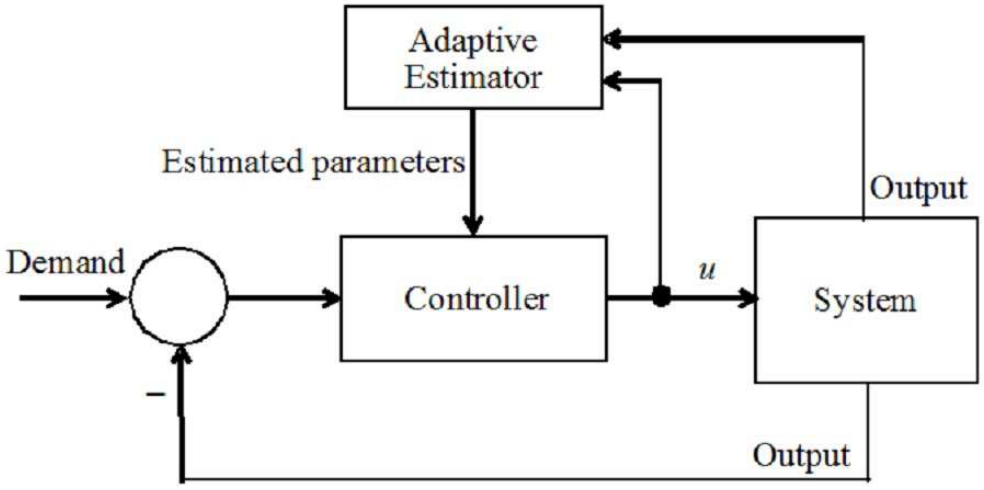

Figure 16 Self-tuning Adaptive Control [18]

2.5.7 Neural Network Adaptive Controller

The knowledge of regression matrix is a problem for classical adaptive controller that makes the overall process lengthy and time consuming. The technique is also demanding with regards to computational resources. In neural network adaptive controller instead of regression matrix the neural network weights matrix is used. The exact

knowledge of these weights is not required and the controller itself adjusts the weights according to the system output by learning from the error in the output.

The learning capability of the neural networks reduces the toll of knowing the parameters during the design phase. Neural networks exhibit universal approximation capability which makes it suitable for any type of control problem irrespective of the model. Neural networks have also been used as hybrid controllers with different layers performing some specific control tasks. An example from [19] is given below with neural network layers being used as components of fuzzy controller.

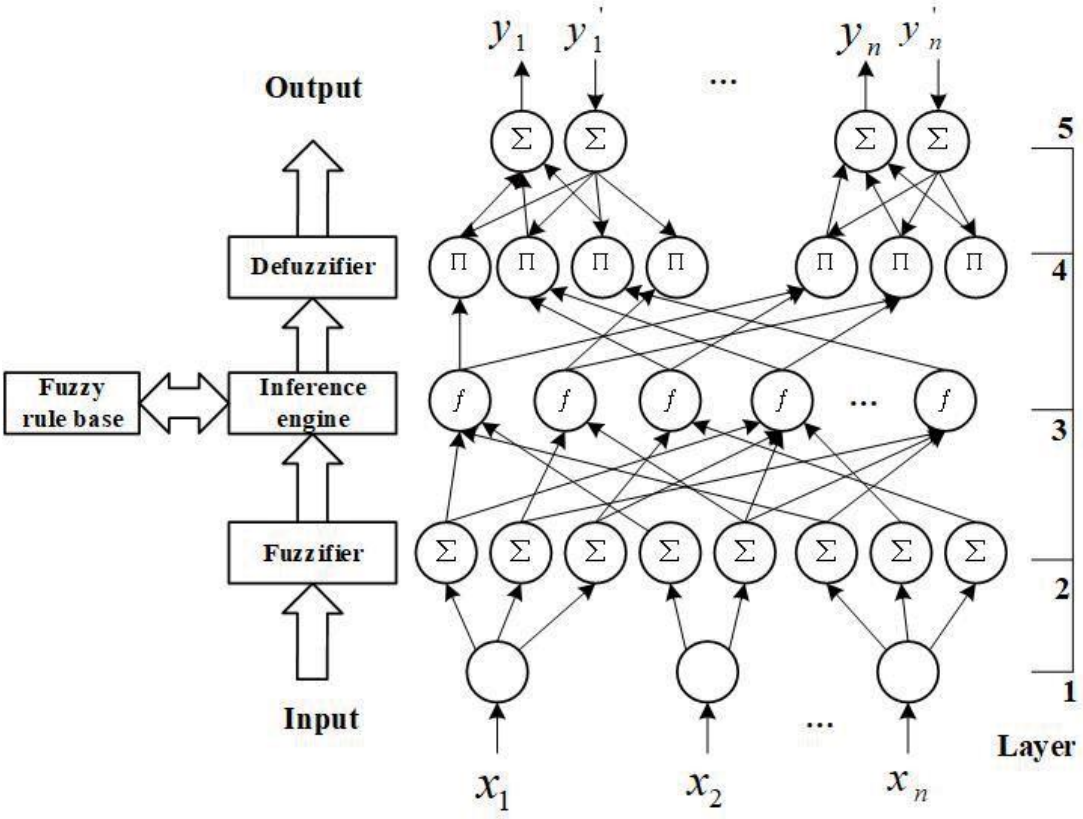

Figure 17 A neural network-based hybrid control for implementing fuzzy control [19]

2.5.8 Analytical Fuzzy Controller

A major drawback of the conventional fuzzy controller is that with increase in the number of input output system variables the number of behavioral rules increase exponentially [15]. This is a major drawback of the controller since it makes the system

computationally demanding for multivariable systems such as robots. This problem is addressed by analytical fuzzy controllers.

The analytical fuzzy controllers use analytical functions to identify the center points the output fuzzy sets instead of basis function definitions. This allows direct mapping from non-linear input variables to the centers of fuzzy output sets. These can be simply implemented in the algorithm.

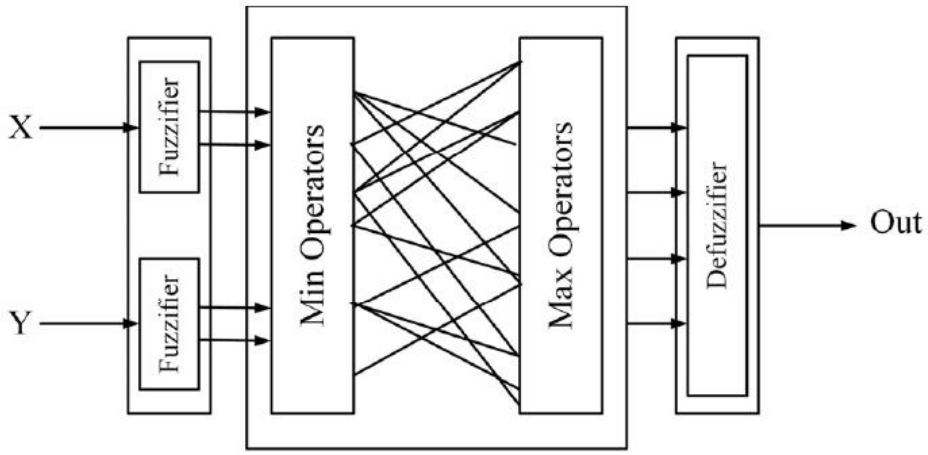

Figure 18 Components of a typical fuzzy controller [19]

2.6 Experimental Implementations

Fuzzy PI controller combined with equivalent control model and deviation coupling model is used in [20] for an instrumented wheelset calibration testbench. The controller manages the PI parameters for control of servo motors for the free wheel and the following wheel based on the position error in the free wheel.

[21] discusses trajectory tracking control that employs fuzzy controller for fuzzy PI parameter self-tuning. The controller has the accuracy of PI controller with the ability to handle non-linear object and model inaccuracies.

AC Servo motor pulse control for accurate position control is implemented in [22]. The authors study the bi-directional position control with speed regulation using PLC configuration software. A simple pulse generator is utilized in [23] for control of servo motors actuating a Stewart platform.

Authors in [24] have developed a trajectory tracking control system, and real time track following is implemented using DOBOT robot. STM32 32bit ARM controller is

used to process the data entered using EU-TFT3.2 touch screen color display. An API is developed in the controller to communicate with the user through touch screen. The controller accepts Bluetooth and Wi-Fi communication protocols to process the signal generated from the capacitive touch screens.

The purpose of trajectory control is to move the end effector of dobot robotic arm according to the provided trajectory. The robot tracking algorithm is developed, and path trajectory is provided using the touch screen. The corresponding motion of robot is physically observed using the drawing pen fixed to an end effector and the position of end effector is observed on computer as shown in figure.

Figure 19 Touchscreen for input, end-effector tracking and attached computer screen [24]

Authors in [25], discuss the use of a PID cascade controller for the trajectory tracking control of a quadrotor. The PID controller is used for the position and attitude control. The control laws are derived with the assumption that the velocities and accelerations are small. The authors have developed a Simulink model for testing controller performance in different path tracking scenarios. Although in literature the use of linear quadratic controller or backstepping and sliding mode controller have been used in control for quadrotors, this paper demonstrates the use of PID because of its simplicity.

Initially the required changes in vertical force of the quadrotor to follow the required hovering height and the required attitude angles are determined by the position controller based on the position error. The attitude controller then calculates the changes in motor speeds required to compensate for the error in attitude.

The position control is managed by the PID controller whereas the attitude control is established by the PD controller at the desired hovering point. Integral control is not necessary for the attitude control since the input for attitude control is the position controller's output which is already PID compensated by the position controller.

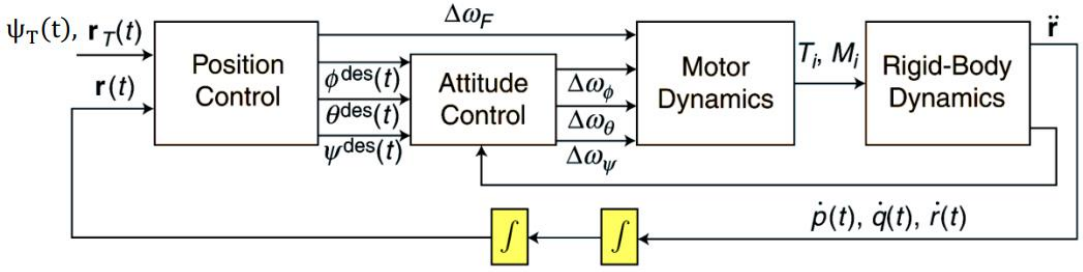

Figure 20 Nested control loops for position and attitude control [25]

The PID controller controls the commanded acceleration based on the errors in position. The position in horizontal plane is controlled by using the pitch and roll error while the error in yaw angle and hover height is used to control the position in vertical axes.

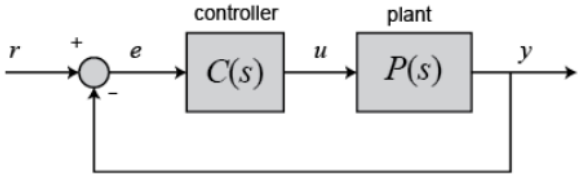

Figure 21 Transfer function for PID tuning [25]

The criterion for the PID controller design is based on minimization of integral of the time-weighted absolute error. The parameters for the controller are determined by comparing the close-loop characteristic equation against the against the characteristic equation of the control criterion. These parameters thus provide the starting values which are later tuned by trial and error. The settling time is chosen so that the attitude controller is 10 times faster than the position controller.

Different experimental schemes have been designed for testing of the quadrotor. The controller performance is evaluated for sinusoidal motions in the single axis for all

three axes. Similarly, circular motion in three planes is performed and controller performance is evaluated for desired vs actual trajectory.

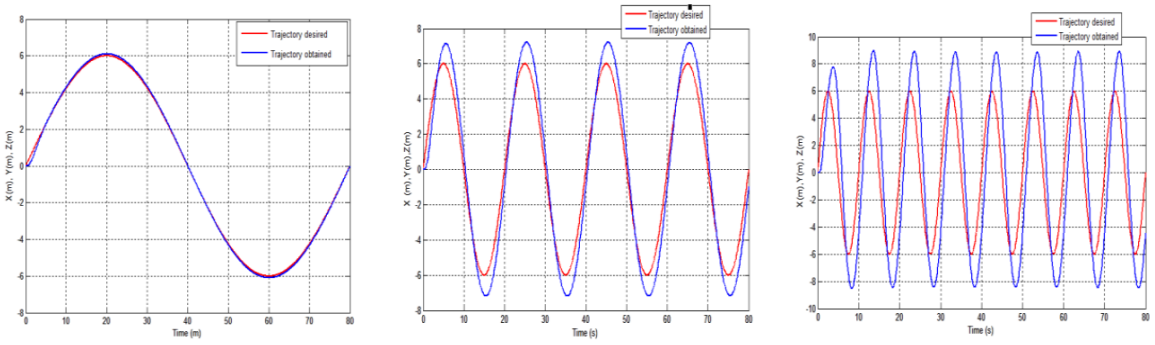

Figure 22 Sinusoidal trajectory tracking with (a) 80s, (b) 20s and (c) 10s [25]

Authors in [26] have developed a leg prosthesis testing robot with 2 degree of freedom motion tracking capability. The robot in the paper is designed for testing of a transfemoral prosthesis. The project utilizes a passive knee with a blade foot. Although active or powered prosthesis can also be attached and tested. A treadmill with the belt driven at speeds manually synchronized with those of the foot is utilized.

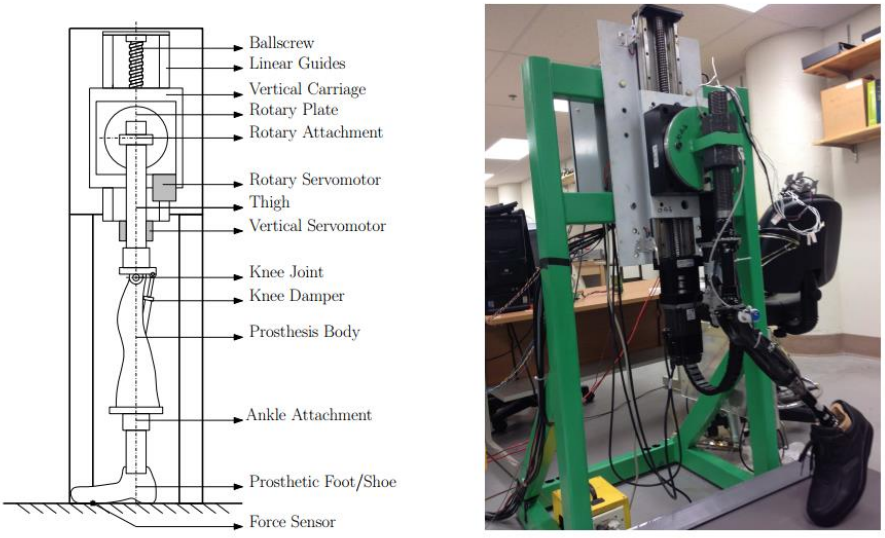

Figure 23 Prosthesis test robot schematic and installation [26]

Electromechanical actuation has been preferred over hydraulic due to accuracy in position control and response possible with such devices. The robot is capable of force control, hybrid force/trajectory control as well as impedance control. Experimental

evaluations in this paper employ, however, a pure motion tracking algorithm. The control problem is to track the motion of hip and thigh to perform the complete gait cycle based on the data gathered by [6] Independent-joint controller is utilized to accurately track the motion profiles.

Single-input single output (SISO) servo loop rotary actuator is used to control the rotary actuator since it is non-back-drivable.

A sliding mode controller is utilized due to its robustness and simplicity in implementation. Single-axis linear actuation model is used for each joint while neglecting inertial coupling. Initially the ability of the robot to track motion profiles is tested without taking force profiles into account. Then, the robot is tested under the application of force by gradually landing the foot on a treadmill and observing force profile till the force exceeds 450N.

The results show only partial compensation of the applied ground reaction force by the controller as expected with the implemented scheme. Tracking error can therefore be observed in the hip vertical displacement and thigh angle during ground contact.

[26] uses following model for each joint,

$$J\ddot{\theta} + b\dot{\theta} = ku + \tau_d$$

where θ(t) represents the controlled position, u(t) is the control voltage assuming proportional relationship with motor torque, the constant k reflects a combination of servo amplifier gain, motor torque constant and rotary/linear motion conversion, J is the inertia of the load and motor, and b is a viscous damping coefficient.

Miroslaw [27] developed the trajectory tracking control of a holonomic manipulator on a non-holonomic platform with external force compensation. The paper discusses problems in the task space finite time control. The manipulator end-effector is susceptible to disturbance forces. Friction forces are also observed at joints that are directly driven by actuators. Moreover, unstructured forces arise as a result of kinematic singularities occurring trajectory execution.

In order to handle external disturbance forces the author has proposed obtaining an estimated extended transposed Jacobian class of controllers. A non-singular terminal sliding manifold (TSM) with a suitably defined task space successfully counteracts the

external disturbance forces based on Lyapunov stability theory. A second-order sliding technique based proposed robust control law is utilized to counter chattering effect. Sliding mode is known to exhibit precision and resistance to disturbances. However, first order sliding mode has a major disadvantage of undesirable chattering. The presented TSM utilizes the first order sliding mode for finite time control in combination with the second order sliding mode responsible for generating continuous control. The controller utilizes a dynamical calculated torque approach and appears to effectively manage trajectory control while efficiently counteracting unknown external forces.

The proposed control technique is proved to be finite time stable based on an assumed criterion. The controller is also energy efficient. This is achieved by removing the need for estimation of the external forces as well as by not requiring the calculation of pseudo-inverse of the Jacobian matrix. Transpose of the estimated Jacobian matrix is used instead. The Lyapunov stability is proved based on practically applicable assumptions. Simulations prove the controller to be more accurate than the current applicable control schemes.

Hongjun [28] proposes a modified linear active disturbance rejection controller (MLADRC). The proposed controller aimed to rectify the problems associated with the model uncertainties and dynamic coupling while rejecting external disturbances. The proposed controller is compared with the proportional-derivative (PD) controller as well as the regular linear active disturbance rejection controller (LADRC).

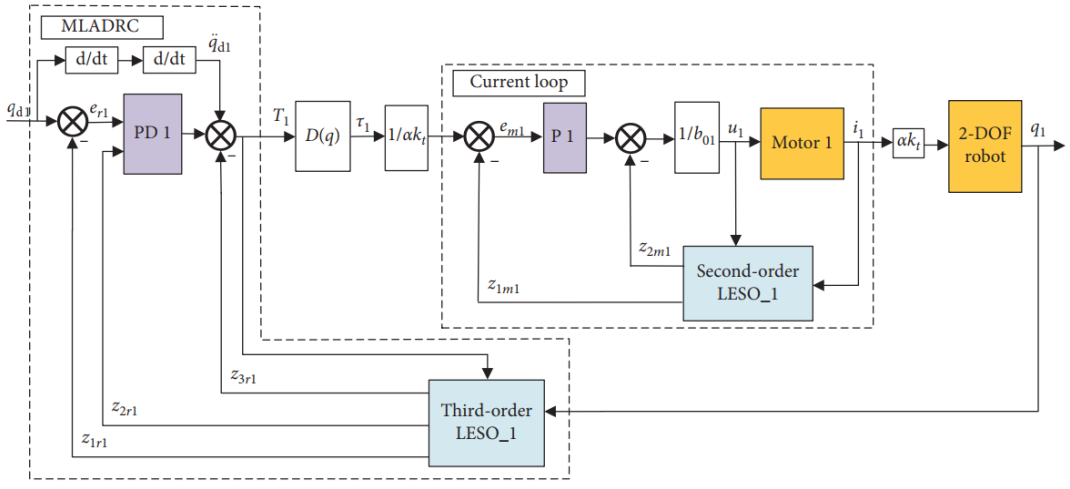

Figure 24 MLADRC trajectory tracking control structure for joint 1 [28]

Actual robot manipulator system is simulated by sequentially adding friction, parameter perturbation and external disturbances. Performance of the MLADRC controller is verified by constructing a 2 degree of freedom (2-DOF) manipulator. The addition of feed forward control of reference angular acceleration is the major difference between the LADRC and the MLADRC. This angular acceleration reference enables a more accurate tracking of target trajectory by the robot manipulator.

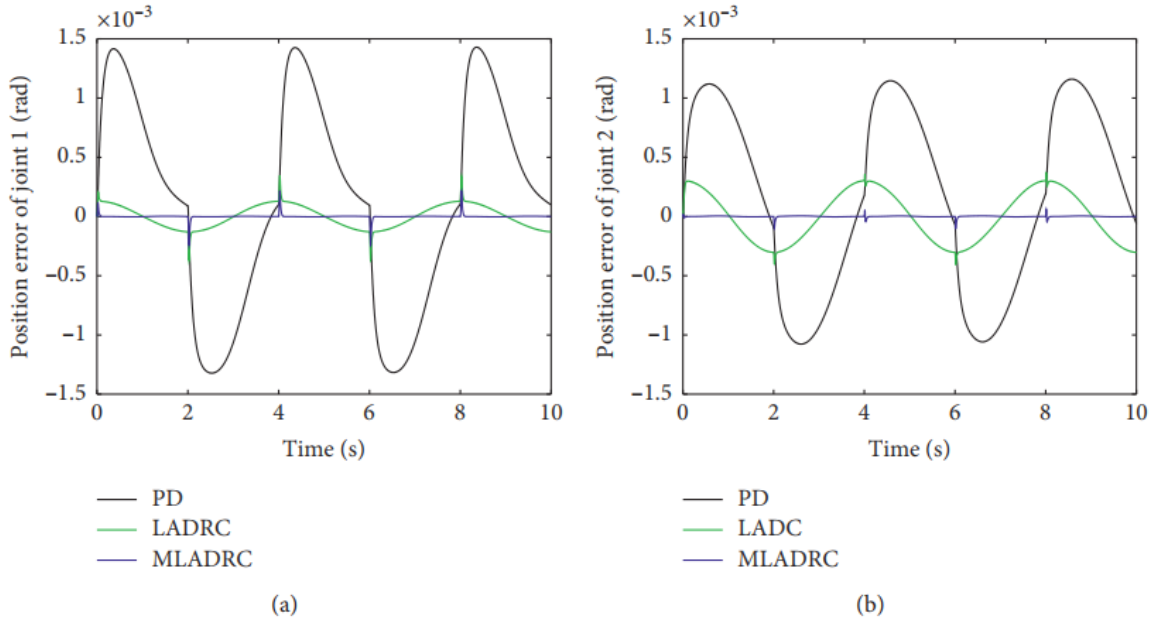

Figure 25 Joint tracking errors with parameter perturbation and friction for PD, LADRC, MLADRC comparison [28]

The paper elaborates the difference between the motion control and dynamic control. Whereas the motion control only works on the negative feedback control of the deviation between the target position and the actual position. The dynamic control works on the dynamic characteristics of the robot. The authors have discussed the different control schemes such as proportional integral differential (PID) control, the iterative learning control, the adaptive neural network control, the sliding mode control and the active disturbance rejection control.

The results indicate a comparison between the position control achieved by PID, LADRC, and MLADRC. The control performance of the MLADRC is verified to be accurate, robust with strong error convergence and excellent disturbance rejection.

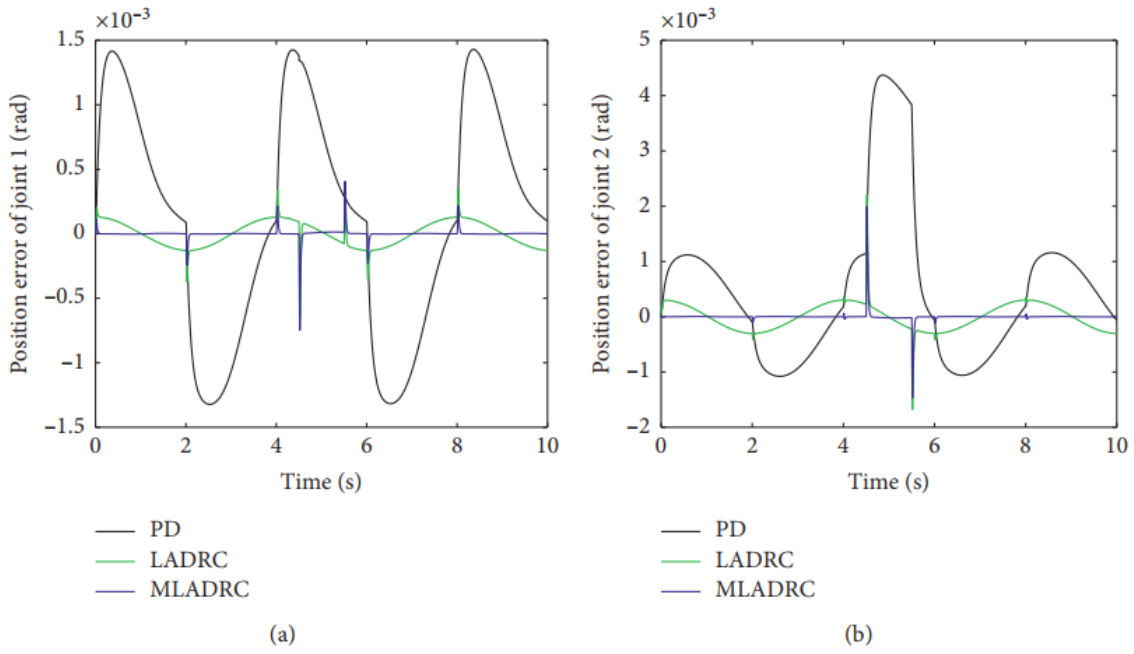

Figure 26 Total disturbances for both joints with PD, LADRC AND MLADRC [28]

The study of literature has provided many effective approaches towards the control of 2 DOF robotic link. In this project the appropriate control scheme has been chosen based on the capability of the selected hardware.

The following chapter explains the methodology adopted for the project. The hardware chosen is first detailed followed by software tools used and finally the control scheme adopted.

CHAPTER 3: METHODOLOGY

This chapter is about the methodology adopted for the implementation of the project. First the hardware is explained in detail. Then the software is discussed and finally the control strategy is explained.

3.1 Hardware

The main hardware components include the testing platform, the AC servo motor and drives, the electronics required for power and interface, and finally the control hardware.

3.1.1 Testing Platform

Figure 27 Prosthesis testing platform

The testing platform is a steel structure placed on the floor. This structure incorporates a carriage that moves along the vertical axis. The vertical motion is enabled

by a lead screw for which the nut is attached to the carriage base. The screw has a lead of 10mm. The lead screw is coupled with a gearbox having a 5:1 ratio. The gear is driven by an AC servo motor. The carriage itself houses another AC servo motor with an attached 80:1 ratio gearbox. The gearbox output shaft has a bracket attached to it for mounting the prosthesis.

3.1.2 AC Servo Motors

Two AC servo motors are attached to the testing platform. Both these motors belong to the Mitsubishi Electric HF-KP Series of AC servo motors.

Figure 28 HF-KP73 AC servo motor for vertical motion of carriage

The vertical motion of the carriage is achieved by HF-KP73, a 750W AC servo motor with 7.2 Nm rated torque. The motor has a quadrature encoder attached to its shaft and housed within the servo motor package. The resolution for the encoder is 18 bits. The encoder thus generates 262144 pulses during one complete revolution. The motor package also has a 24VDC brake. The brake is disengaged when 24V are applied to the relevant power lines. The servo motor has a rated speed of 3000 rpm. A maximum speed of 6000 rpm can be achieved.

The motion for the thigh is achieved by HF KP 43, a 400W AC servo motor with a rated torque of 3.8 Nm. Like the motor for vertical motion, the thigh servo motor also

has an encoder with 18 bits of resolution. The motor has 3000 rpm rated speed and 6000 rpm of maximum speed.

Figure 29 HF-KP43 AC servo motor for angular thigh motion

3.1.3 AC Servo Drives

The AC servo motors are driven by two Mitsubishi Electric MR-J3 Series AC servo drives. The servo drive for the vertical axis motion is the MR-J3-70A. The drive for the thigh motion is MR-J3-40A.

The servo drives require 220V AC for the main circuit and base circuit power. The control circuit is driven by 24V DC power. Each drive has a minimum emergency and power logic circuit requirement which is detailed in the relevant manual. The details are also available in the appendix.

The servo drives have 3 modes of operation.

a. Position Control Mode
b. Speed Control Mode
c. Torque Control Mode

For this project the drives have been configured for position control mode. The position control mode allows the position to be achieved by sending exact number of pulses equal to the difference of target position from the current encoder position.

The servo drives are driven by the control inputs in the form of differential pulse train from the motion controller. The pulse train is provided to the two differential pair inputs (PP, PG and NP, NG) on the motion control input interface of the servo drives. The PP, PG differential pair pins are supplied with the pulse train for the forward motion while the reverse motion is achieved by applying the pulse train to the NP, NG pair pins on connector CN-1 of the drives.

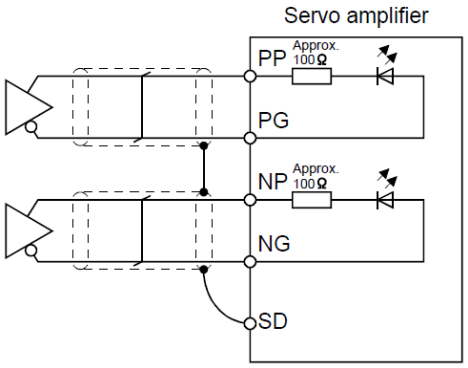

Figure 30 Servo drive differential interface for pulse train (MR-J3 Datasheet)

The drives have the capability of electronic gearing. This feature enables high speeds at low input frequencies. Thus, the output frequency of the controller does not have to be very high. However, this feature is to be used in accordance with the required control accuracy.

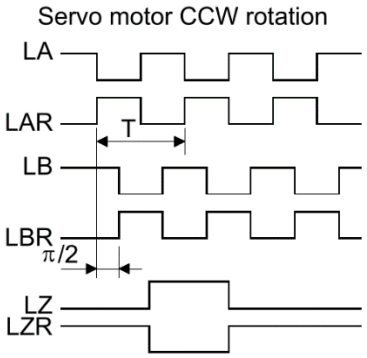

Figure 31 Encoder output pulses (MR-J3 Datasheet)

The encoder feedback for the motion is provided by the drives to the controller in the form of differential signals. These signals are the pairs LA, LAR for channel A, the LB, LBR for channel B. Another pair the LZ, LZR provides a pulse once per revolution. The signals A and B are out of phase by angle π/2. The drives encoder output can be configured to provide a given number of pulses for channel A and B during one revolution.

The configured number in this project is 4000 pulses per revolution (ppr). The MR-J3 Servo Drive manual provides the necessary information for configuration.

Figure 32 MR-J3-70A AC servo drive

Figure 33 MR-J3-40A AC servo drive

3.1.4 Power and Emergency Cut-Off Circuit

A power and emergency cut-off circuit is provided to power the AC servo motor drives for the attached motors. The circuit has 220V AC power for the AC servo drives. There is a power breaker and magnetic contactor for each of the two servo drives. The circuit also has 24V and 5V DC power supplies for the associated control circuitry. The 24V DC is employed to power the control circuit within the AC servo drives. Also, the brake on the vertical drive motor requires 24V DC for actuation. On board relay logic

handles the emergency and control requirements for both the AC drives. The circuit has start, stop and emergency stop switches for the power supply ON and OFF controls.

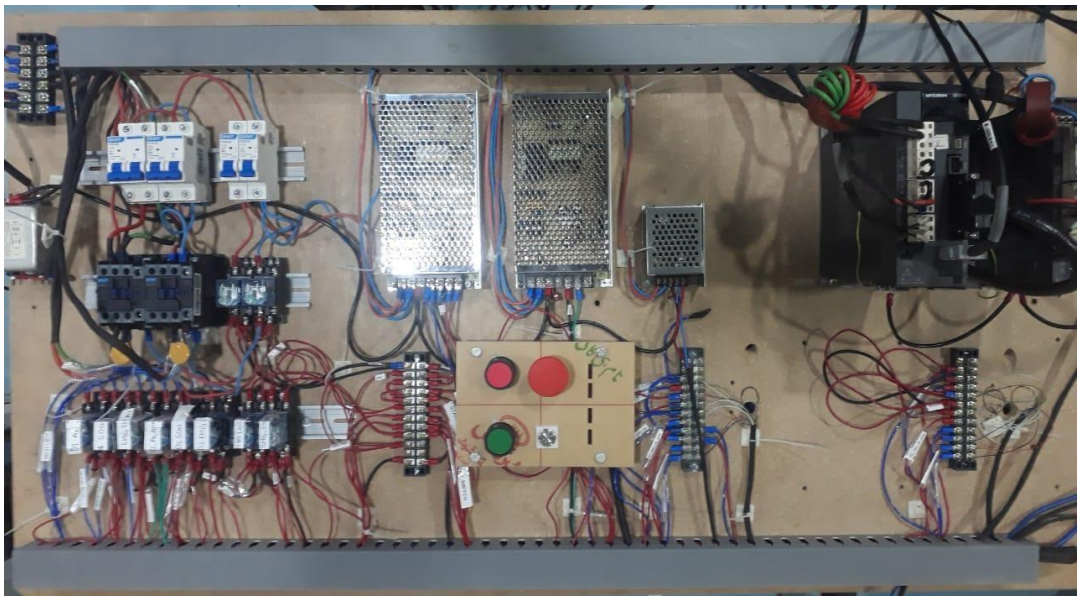

Figure 34 Power and Emergency cut-off circuit

the power cut-off circuit is in accordance with the data provided by Mitsubishi Electric in the servo drive manuals. The manual provides the circuit for one unit installation. However, in this project two drives have been connected so that the alarm and emergency situation for any one of the drives will disable the output of both drives to avoid any accidents.

The figure above shows separate breaker and magnetic contactor for each drive in the top left. A third breaker supplies AC power to the 24V and 5V DC power supply units. One of the two 24V supply is for the drive control circuit while the other one is for the brake of the vertical axis motor.

3.1.5 Motion Controller

The motion control is performed by the STM32F407 Discovery board. The motion controller has a 168MHz clock operation which enables efficient performance of the onboard peripherals. The motion profiles for the hip and thigh as per the human gait dataset are downloaded to the motion controller from a PC Supervisor. The hardware

generates the necessary signals through the interface electronics to perform the actuation of the two motors.

Figure 35 STM32F407 Discovery Board

The controller has two onboard 32-bit timers used in encoder mode for highspeed encoder position input capture. One timer is utilized for each encoder input in quadrature mode also known as X4 mode. The output is generated by utilizing 16-bit timers in PWM modes. One 16-bit timer is dedicated for each servo drive. Two PWM channels of each timer, one for the forward and the other for reverse pulse train generation, are used.

3.1.6 Interface Cards

The interface between motion controller and servo drives is provided by two interface cards. The interface cards are powered by the 5V DC power supply available onboard the Power and Emergency Cut-off Circuit. Each Interface card has an onboard 5V to 3.3V power converter and the logic level translators between 5V and 3.3V. The 5V DC powers the onboard AM26LS31 single line to differential drivers as well as the AM26LS33 differential to single line drivers. The logic level translators utilize both the 5V and 3.3V supply inputs.

The interface card has 4 output channels for the command pulse pairs. These channels are attached to the drives PP/PG and NP/NG contacts of the servo drive. Two out of the four differential outputs of AM26LS31 are used as the command pulse interface. The input of each AM26LS31 are the two single line connections from the motion

controllers PWM output pins. One line is for forward motion while the other line is for reverse.

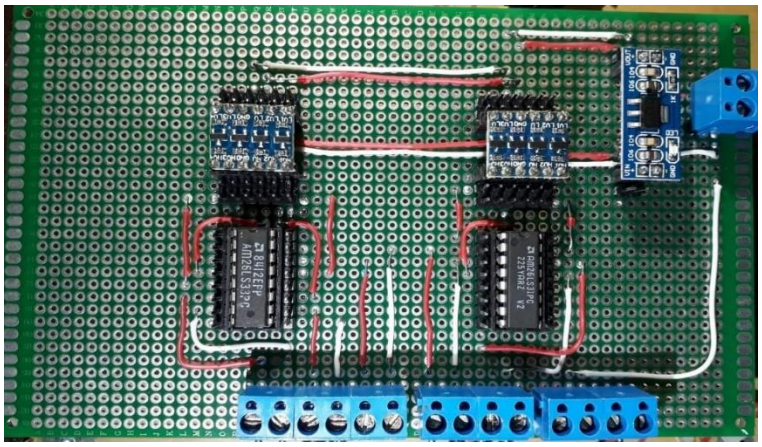

Figure 36 Interface electronics for encoder input and drive pulse command

The logic diagram for the AM26LS31 single line to differential driver as given in the datasheet are shown. The channels xA are the inputs whereas the signals xY and xZ are the differential outputs where x represents the channel number from 1 to 4. G and its complement are the enable signals for the IC.

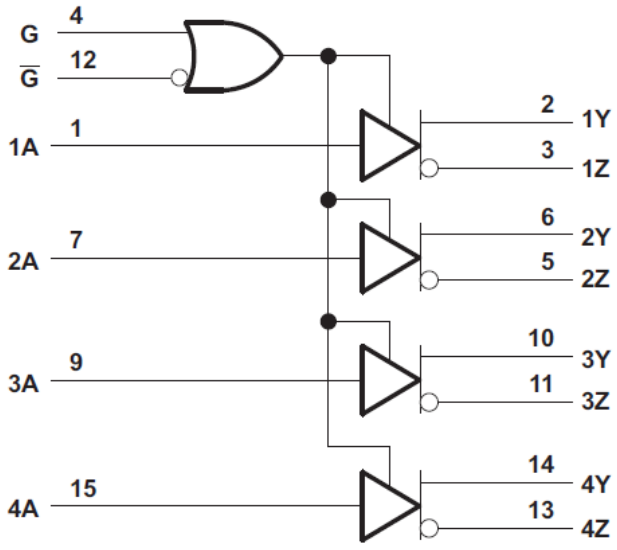

Figure 37 Texas Instruments AM26LS31 logic diagram

The encoder signals are received at 6 input channels, two for each differential pair. The AM26LS33 ICs receive the differential input and convert to single channel outputs. Logic diagram for the IC provided in datasheet is given below.

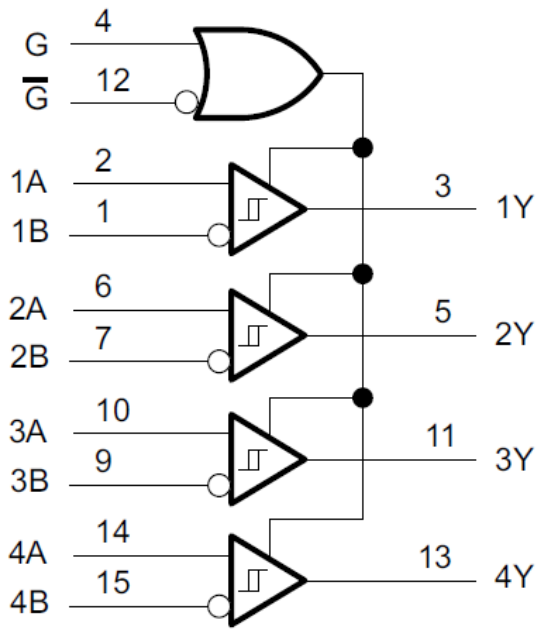

Figure 38 Texas Instrument AM26LS33 logic diagram

Here the signals xA and xB are the differential input signals and xY represents the output where x is the channel number. The input to the AM26LS33 is the encoder channels LA/LAR and LB/LBR connections from the servo drive. The output of AM26LS33 differential to single line are connected to the pins associated with 32-bit timers of the motion controllers.

3.1.7 PC Supervisor

The supervisory hardware is personal computer (PC) or a laptop with MATLAB software installed. The hip and thigh gait data profiles are loaded from the dataset and visualized in the MATLAB. The PC communicates with the motion controller to download the hip and thigh motion profiles. The motion results can also be communicated back to the PC from the motion controller. The communication is performed on RS-232 serial interface at 115200 baud.

3.2 Software

The system has the software in two locations. The supervisory software has MATLAB code that resides on the PC whereas the embedded code for motion control resides in the STM32F407 Discovery board.

3.2.1 MATLAB Code (PC)

The MATLAB code enables the loading of hip and thigh motion profiles from the gait dataset. The loaded data can be visualized on screen. The data can then be downloaded to the motion controller for executing the motion profiles. The visualization of the performed motion output can also be viewed.

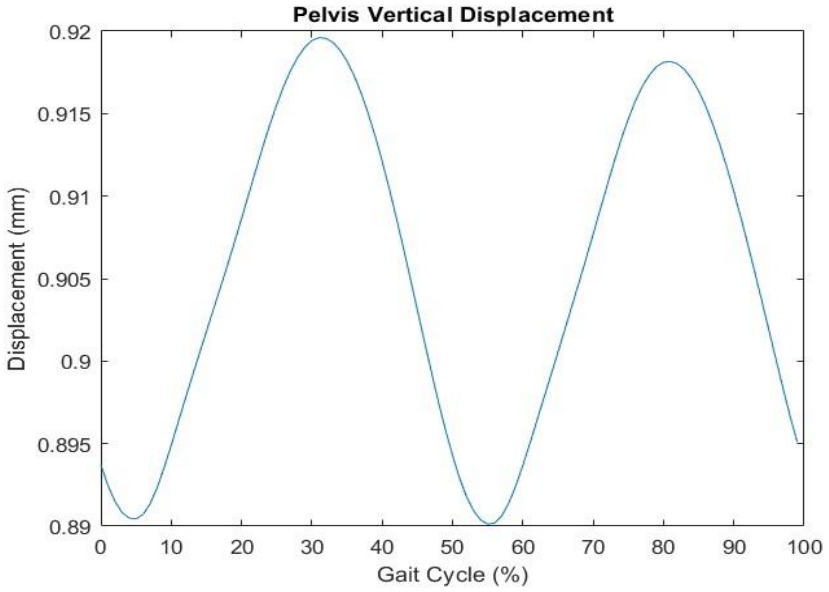

Figure 39 Motion profile of pelvis in z axis

The MATLAB code extracts the 100 points data from the mean data in the original dataset. The data is now in the form of two matrices. One of these matrices is the hip data and the other is the thigh angle. The first column of each of these matrices is the gait cycle percentage. The second column in case of hip profile matrix holds the data for the hip vertical position in meters. The position is the absolute position of the hip in meters from the ground.

The height offset is removed from the data by subtracting the minimum value in the column from all values. The offset can be added later according to configuration of the prosthesis on the platform. Similarly, the second column in the thigh profile matrix

contains the thigh angle in radians against each gait cycle percentage. This data is kept unchanged to keep the thigh angle as per original data set. The matrices have the gait percent in integer datatype form and the position value as a floating-point number form.

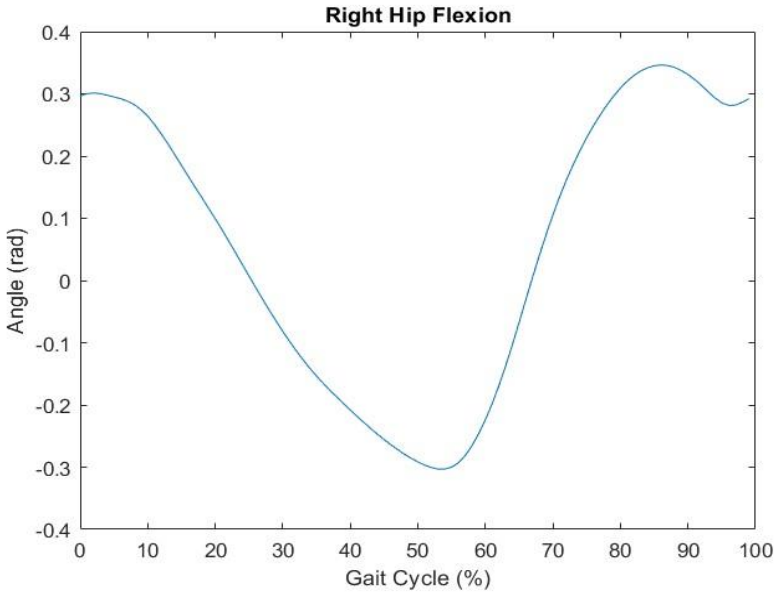

Figure 40 Hip flexion profile of right leg

To communicate this data to the motion controller the data is converted to string and each matrix is passed on to the serial buffer in the following format.

Gait Cycle %	Seperator	Data Value
0	,	0.8937

Figure 41 Communication string format

3.2.2 Firmware (Motion Controller)

The firmware resides in the embedded motion controller. The embedded software can receive the two motion profiles i.e., the hip and the thigh motion profile. The received data is in string format and then converted to the original formats i.e., integer format for gait cycle percentage and floating-point format for position. The user can then command the execution of these profiles. Once the execution is started the controller commands the drives to follow the trajectory of the data set.

The current position data from the drive is received on four controller pins associated with two 32-bit timers. Each timer has two pins associated with it. One of these pins is connected to the channel A of the encoder and the other to the channel B. The timers are used in the encoder mode with both timer input channels TI1 and TI2 contributing to the total count. This is known as X4 input configuration. In this mode the rising as well as falling edges on both channels are recorded as ticks in the timer's counter register.

The command pulses for each drive are generated on two separate pins associated with 16-bit timer. Two 16-bit timers therefore drive the whole system. Of the two pins associated with a timer one is for forward direction pulse train and the other for the reverse direction pulse train. The pulse train is generated by using timer in PWM generation mode. One of the PWM channels is thus used for the forward direction and the other for the reverse.

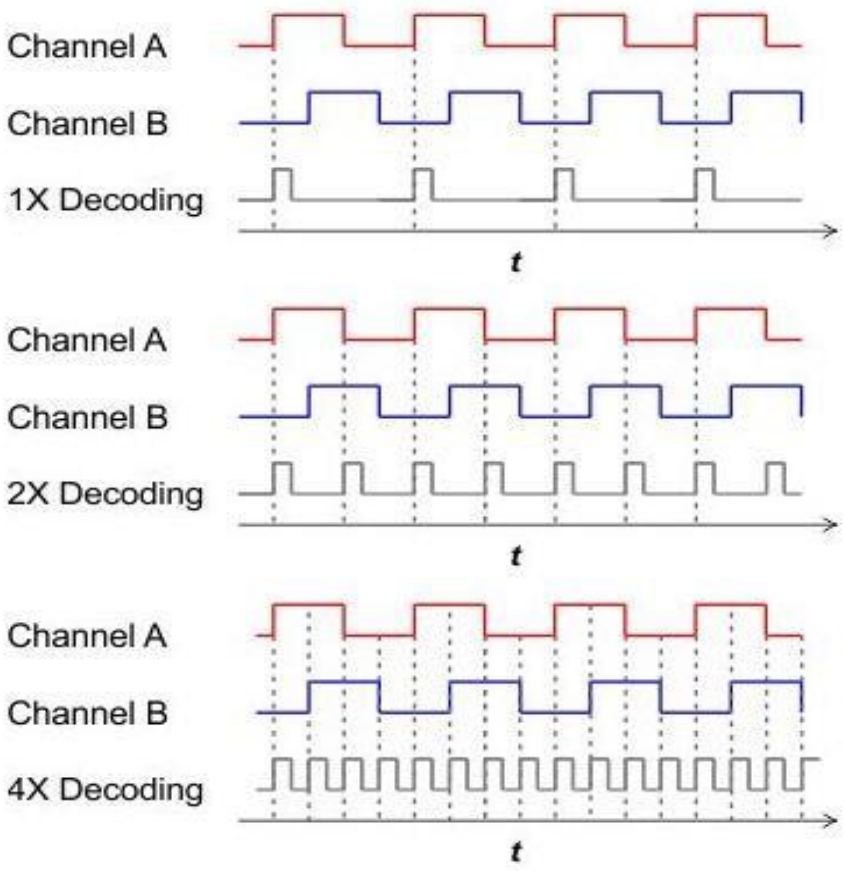

Figure 42 Encoder pulse input configurations

3.3 Control Scheme

The control scheme is shown in the figure above. The gait cycle data is obtained in MATLAB on the supervisor PC. The MATLAB script is used to convert the data points from meters to millimeters for the hip vertical displacement profile. The data points are also offset to change the displacement span from the height of the hip from ground in the actual dataset to the zero reference. This is done so that the motion can be performed at any height as per requirement from the machines ground reference. The data points for the thigh angle is kept unchanged as its reference is the axis of the leg in stance phase.

The data from the supervisor is passed to the motion controller at 115200 baud in the form of 100 strings for each of the two profiles. During reception the motion controller updates the supervisor regarding the successful reception of each of the two profiles.

The controller clock has been configured to run at bus speeds of 84MHz. The timer used for the PWM controller is configured with a pre-scalar value of 84 so that it can produce an increment at 1 microsecond interval.

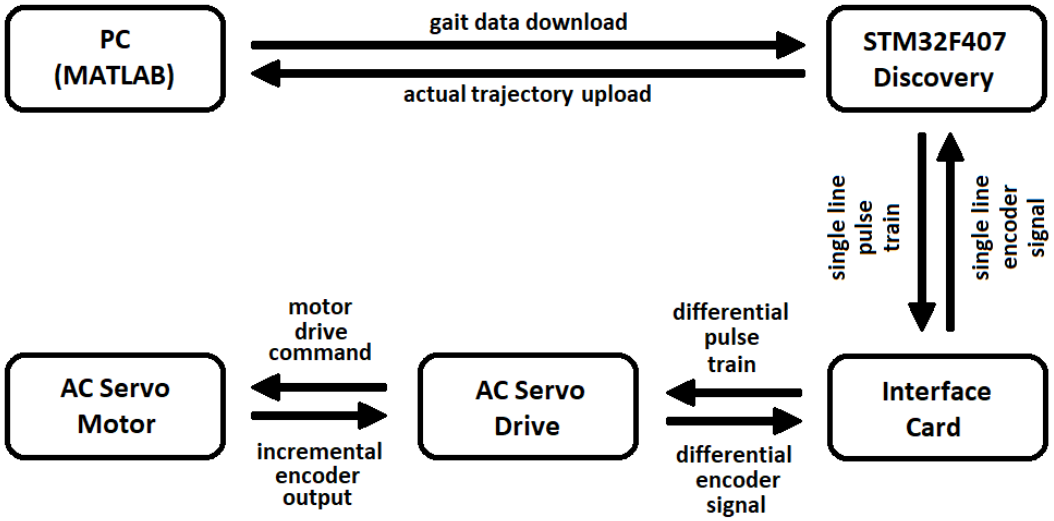

Figure 43 Control scheme for transfemoral testing platform

The motion controller commands the servo drive by generating the pulse command and acquires the encoder position data from the drive.

3.4 Control Algorithm

The controller acquires the two profiles that are required to be executed from the supervisor PC. Each profile contains the 100 points of position data for the hip and thigh motion trajectory. The algorithm has been developed in the form of a state machine so

that the status of acquisition of the two profiles can be viewed on the supervisor PC. The data is stored in the form of two arrays of 100 points each in floating point format.

Once the profiles have been successfully stored the data is further processed creating a set of two more of arrays for each profile. One set of these arrays stores the change in the position between two consecutive trajectory points. This is later used to calculate the velocity in the two axes at each gait cycle point. The calculation of velocity is based on the time for one complete gait cycle. Assume that the gait cycle is to be completed in T_{gc} milliseconds. So, the time duration *t* in milliseconds between successive data points is given as,

$$t = T_{gc} / 100$$

The time *t* is then used as the time base for gait cycle update. The arrays of change in position when divided by the equivalent of this time gives the array of velocity values at each successive gait cycle point. This array is further used to calculate the array of frequencies required to be output at each gait cycle point during execution.

The frequency is calculated for each profile array by incorporating the physical and electronic gear ratios of the system. For example, the calculation of frequency *f* for achieving the speed *n* for the hip at a particular gait cycle point can be calculated as,

$$f = (n / 10) \text{ x gr x ppr / egv}$$

where egv is the electronic gear value configured in the drive, ppr is the encoder resolution and gr is the physical gear ratio of the gear attached to the motor. The value 10 represents the lead of the ball screw in millimeters.

The control loop variable represents the gait cycle point and is also used as the array index. At each gait cycle point the frequency value from the frequency array is inverted to calculate the PWM timer period T_{tm} which ensures the generation of required frequency at each point in the trajectory. This ensures the speed of the hip axis to be as per required value. The controller can therefore command the drive to follow the position and the velocity profile for each dataset. The error in position and velocity of the hip and thigh against each value of the gait cycle percent is then compensated using the PID control technique for handling the pulse frequency.

The thigh motion profile has position value in radians. Like the hip profile the thigh profile also has 100 data points. The calculations for velocity and frequency for the thigh profile are similar to that of the hip profile.

The equation for frequency *f* of the thigh motion is calculated using the formula,

$$f = (n / 2\pi) \text{ x gr x ppr / egv}$$

Where *n* is the speed required in radians per second gr is the gear ratio of the gearbox attached to the motor and egv is the electronic gear value configured in the drive. The frequencies thus generated are transferred using the connected PWM channels and sent to the drives for execution of motion.

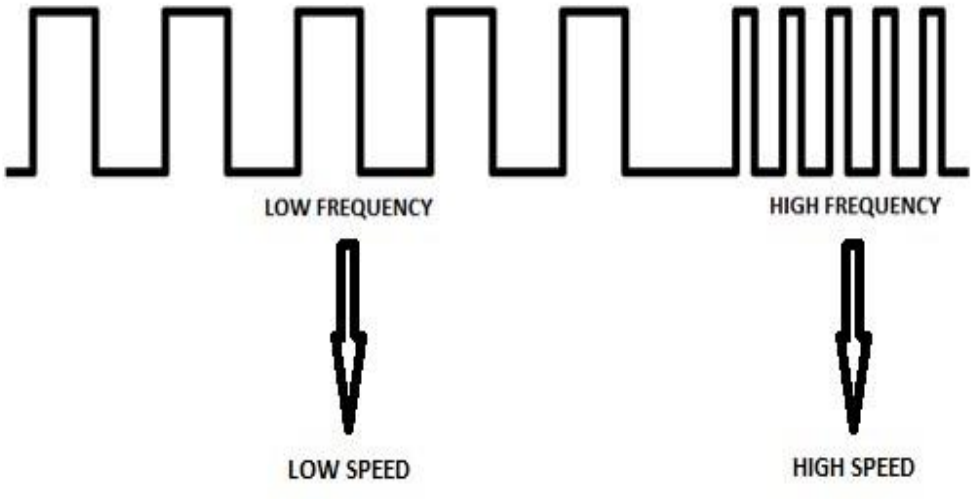

Figure 44 Pulse frequencies for low and high speeds

CHAPTER 4: EXPERIMENTAL RESULTS

4.1 Pulse Generation

Initially the motor for hip motion was tested in no load condition. The generation of PWM and the feedback of the encoder was observed using logic analyzer and visualized on computer. The aim was to view the response of the motor in accordance with the actuation frequencies before the motor could be mounted on the frame.

The actuation algorithm and timer operation were validated by generating a varying frequency from 20 Hz to 4430Hz. The frequency of 20 Hz was checked to produce a jerk free output so that at any time if required the motion could be smooth. The motor was observed to produce a fine motion. The frequency of 4430Hz in combination with an electronic gear of 5917 can produced motor rpm of near 6000.

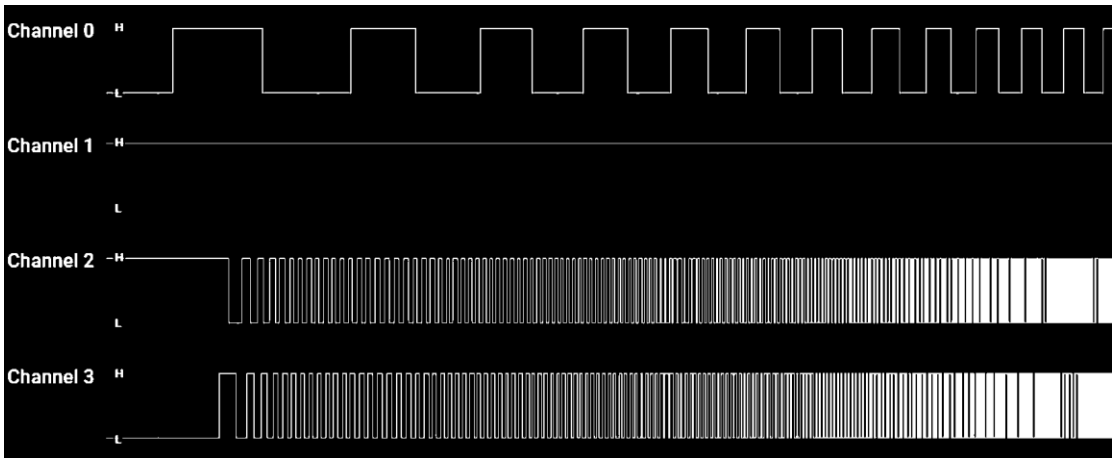

Figure 45 Pulse command with encoder feedback

In the figure above the command pulse train can be seen on channel 0 of the visualization software. The encoder feedback pulses are visible on channel 2 and 3.

4.1.1 Direction Control

After the pulse generation algorithm was found to work fine, the next step was to control the direction of the motor. The PWM channel is required to be switched in accordance with the configuration of the drive to make the motor turn in opposite direction. The PWM channel is switched in way that the frequency is applied for one channel resulting in motion of servo motor in one direction. Then the frequency is applied

to the other channel to make the servo motor in opposite direction. The figure shows the rotation of the motor being switched halfway through the visualization.

Channel 0 presents the initial pulse train. After some time the pulse is switched to the other channel which is seen on channel 1. The change in direction of motion can be verified by the fact that the encoder channel B visible on channel 3 initially leads the channel A feedback on channel 2. Upon switching the channel A starts leading channel B.

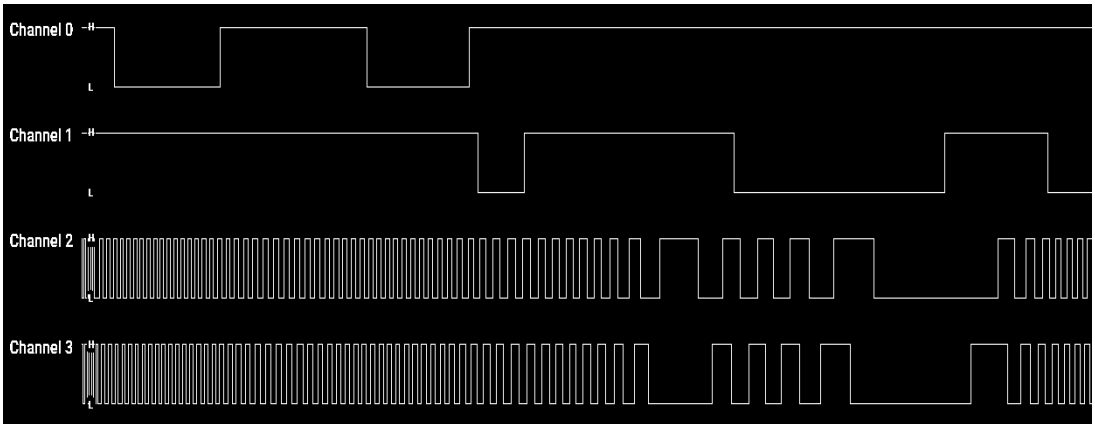

Figure 46 Direction control with encoder feedback

4.1.2 Sinusoidal Pulse Generation

Finally, the last step in unloaded tests is to check the sinusoidal response of the motor. Frequency is varied from 20Hz to 2500Hz at first in increments and then decrements to make the actuation a sinusoidal pattern. When the decrement reaches 20Hz the direction is inverted by switching the PWM channel and the same pattern is repeated. The motor response is found to be accurate. This experiment is important because the gait cycle profile for hip and thigh motion has varying sinusoidal patterns. The results of the sinusoidal motion can be seen in the figure below.

The figure shows increasing and decreasing frequencies on channel 0. This corresponds to increasing and decreasing speed in forward motion. Then the PWM channel is switched, and the frequencies can be observed on channel 1. The corresponding change in direction and changes in speed can be seen.

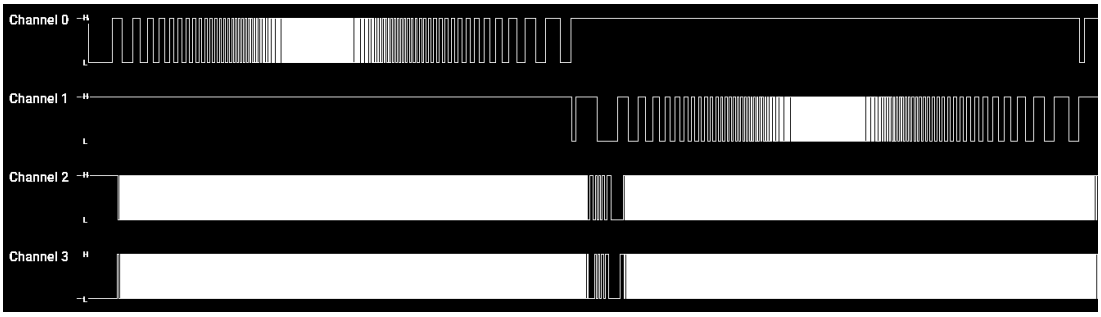

Figure 47 Sinusoidal command with encoder feedback

4.2 Loaded Actuation

Upon completion of initial tests, the system is actuated in loaded state. This is done for each drive with single motor actuation initially and then simultaneous actuation to produce the complete motion of the frame similar to human gait. The response of the system for 5 gait cycles is logged in the motion controller and updated to MATLAB after completion of the sequence for 5 gait cycles. The data received is then visualized in MATLAB.

4.2.1 Hip Vertical Actuation

The tracking performance for the vertical displacement trajectory is shown in the figure above. The target trajectory is found to lead the actual trajectory by a certain amount. This results in the error shown in the same plot in red. The system tracks the target trajectory with this lag but overall the sequence is uniform which indicates the repeatability of the tracking algorithm. The error is bounded indicating asymptotic stability.

The analysis of a single gait cycle is required to evaluate the tracking performance of the system for the particular axis. Given below the system response for the hip vertical displacement during single gait cycle can be seen.

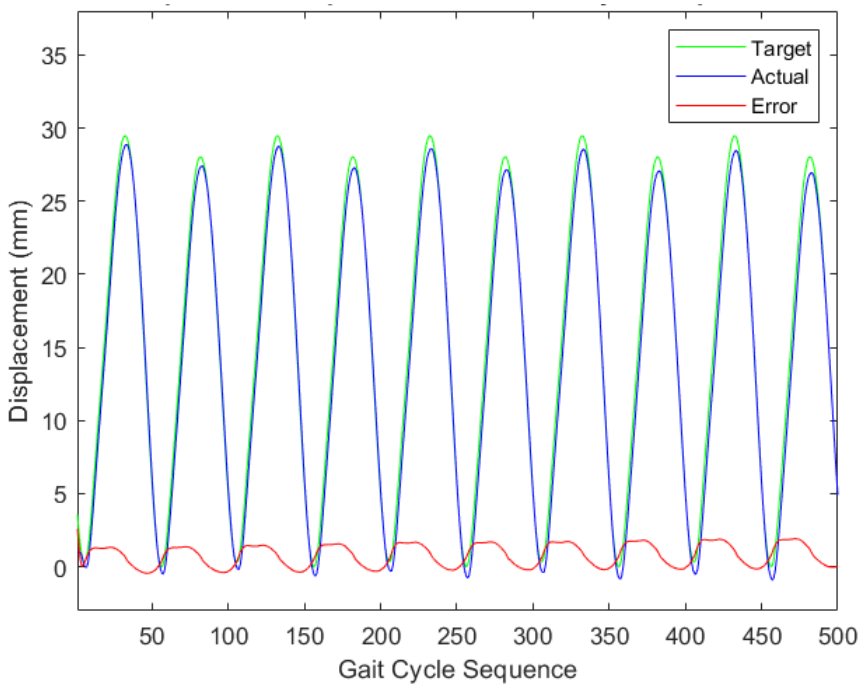

Figure 48 Hip vertical displacement for 5 gait cycles

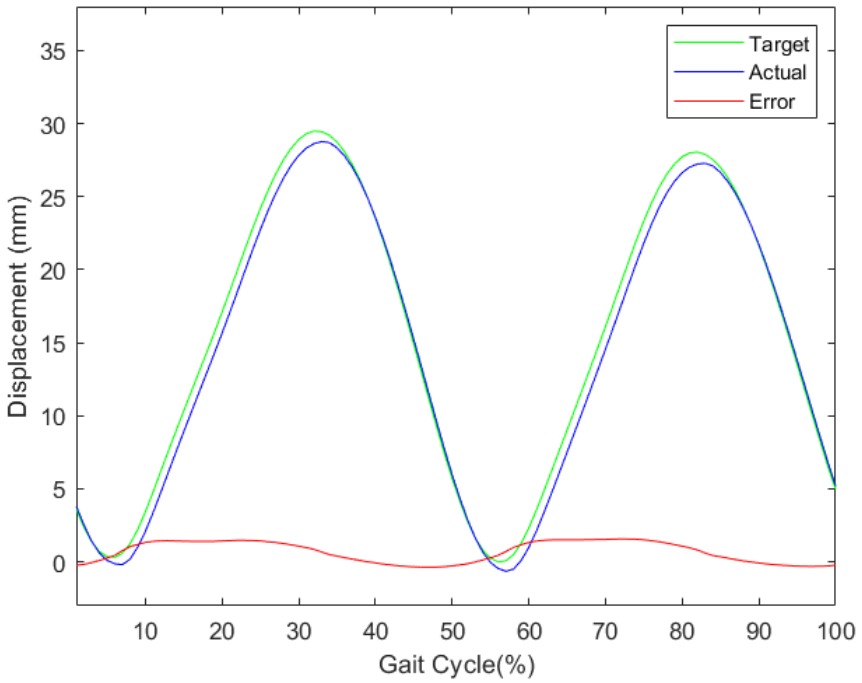

Figure 49 Hip vertical trajectory tracking for single gait cycle

The error in the hip vertical displacement is bounded and can be observed in the plot below. It can be observed the error is more in the positive direction when the system is moving against the gravity than the downward motion.

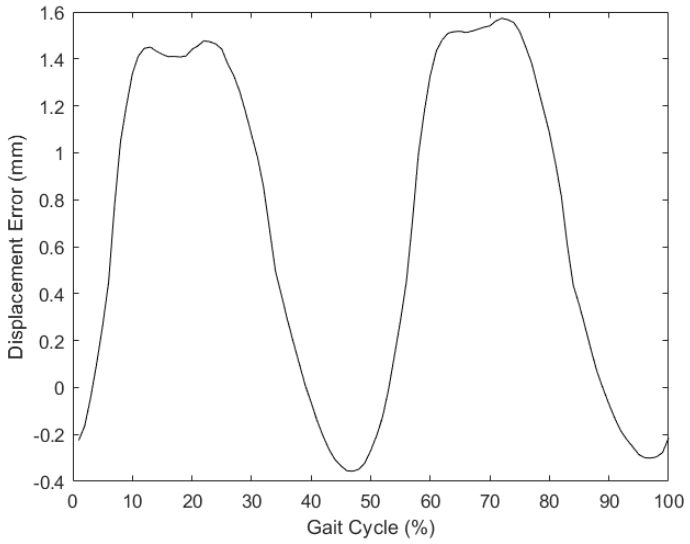

Figure 50 Error profile for hip vertical displacement

4.2.2 Thigh Angular Actuation

The angular motion of the thigh for 5 gait cycles is seen below. The data shows that the behaviour is similar to the hip vertical actuation. The actual trajectory lags the target trajectory by a certain amount. As a result the error at that gait cycle point is non-zero.

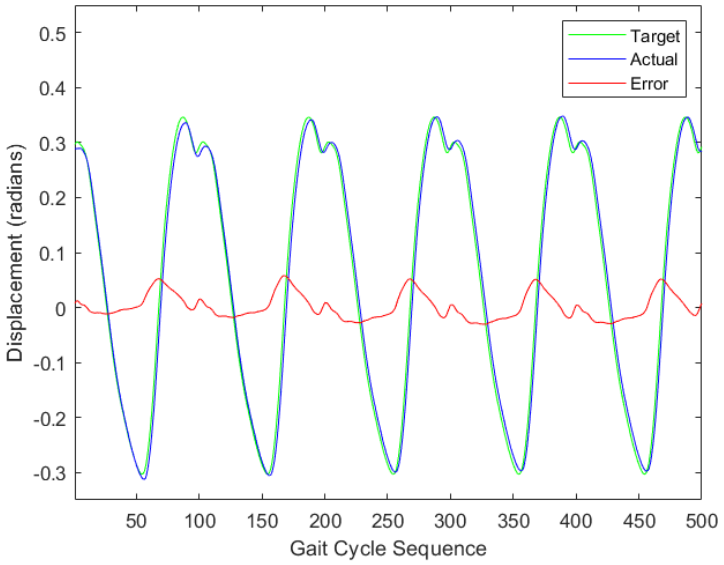

Figure 51 Thigh angular displacement for 5 gait cycles

Like the hip vertical actuation, the thigh actuation results also indicate bounded errors and repeatability. Asymptotic stability of the system is therefore ensured. The response for single gait cycle is shown in the associated figure. The error bounds can be seen in the associated figure.

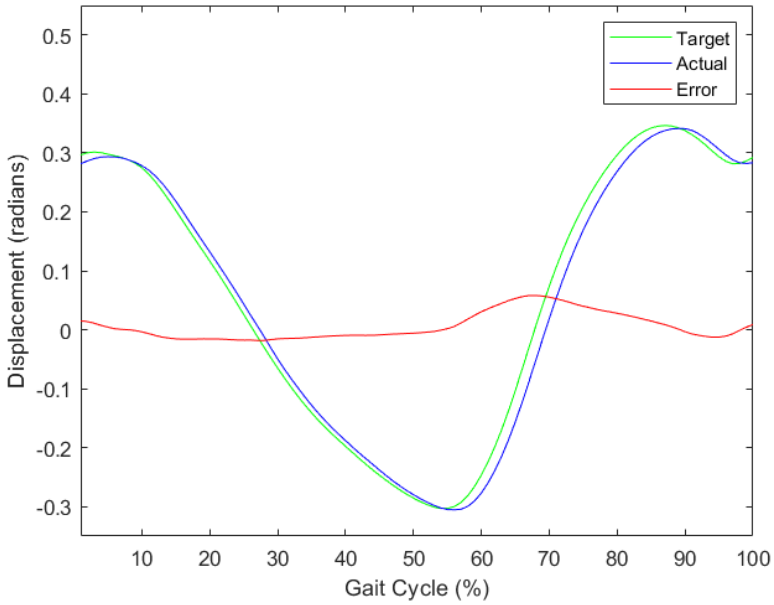

Figure 52 Thigh angular displacement for single gait cycle

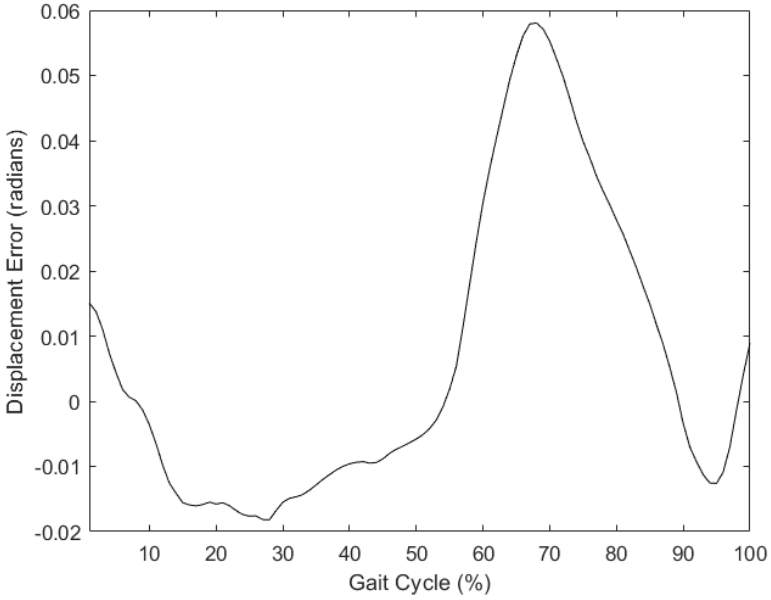

Figure 53 Error profile for thigh angular displacement

4.3 Discussion

This section narrates the analysis based on the results in the previous section.

4.3.1 Repeatability

The system in this project has been developed for performing the cyclic testing of transfemoral prosthesis. The response of the system shows repeatability which is essential or the cyclic testing. The lag in the tracking is symmetric and does not affect the smooth execution of the trajectory thereby rendering the system useful for the intended use.

4.3.2 Effect of Gravity

As learned from the literature review the vertical plane robots are affected by the force of gravity. From analysis of the error curves, it can be seen that the error increases in situations when the motors are actuated against the gravity whereas the error reduces when the motion is assisted by it. This is observable for the hip motion trajectory curves during the upward motion.

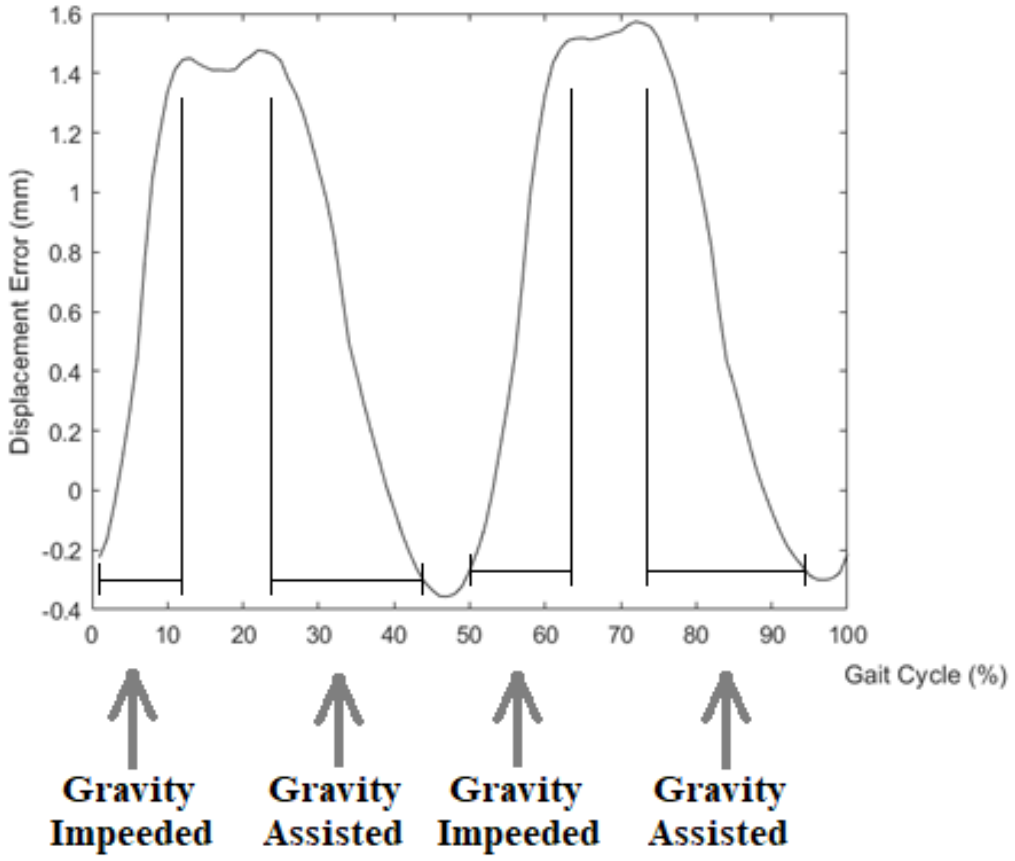

Figure 54 Gravity contribution to hip vertical motion error

Between the 0 to 12 percent gait cycle and again between 50 to 64 percent gait cycle the tracking error tends to increase. During 0 to 12 percent gait cycle the hip is traveling upwards as the stance phase proceeds from initial loading to mid-stance. During this section of the stance phase the motion is impeded by gravity. This is characterized by the increase in the tracking error. During 50 to 64 percent range of gait cycle the hip again travels in the upward direction as this is the stance phase for the other leg during bipedal motion of the human body. Again, the tracking error increases during this period as the motion is again impeded by gravity.

At mid-stance the hip is at the maximum height in the gait cycle. From this point onwards the hip continues to travel down as the gait cycle progresses from mid-stance to terminal stance. This is roughly the period from 20 to 40 percent of gait cycle. During this time the motion is assisted by gravity and the error curve shows a decrease in motion error. A similar effect is observable between 70 and 90 percent of the gait cycle stage. This is the phase when the other leg is preceding from its mid-stance to terminal stance.

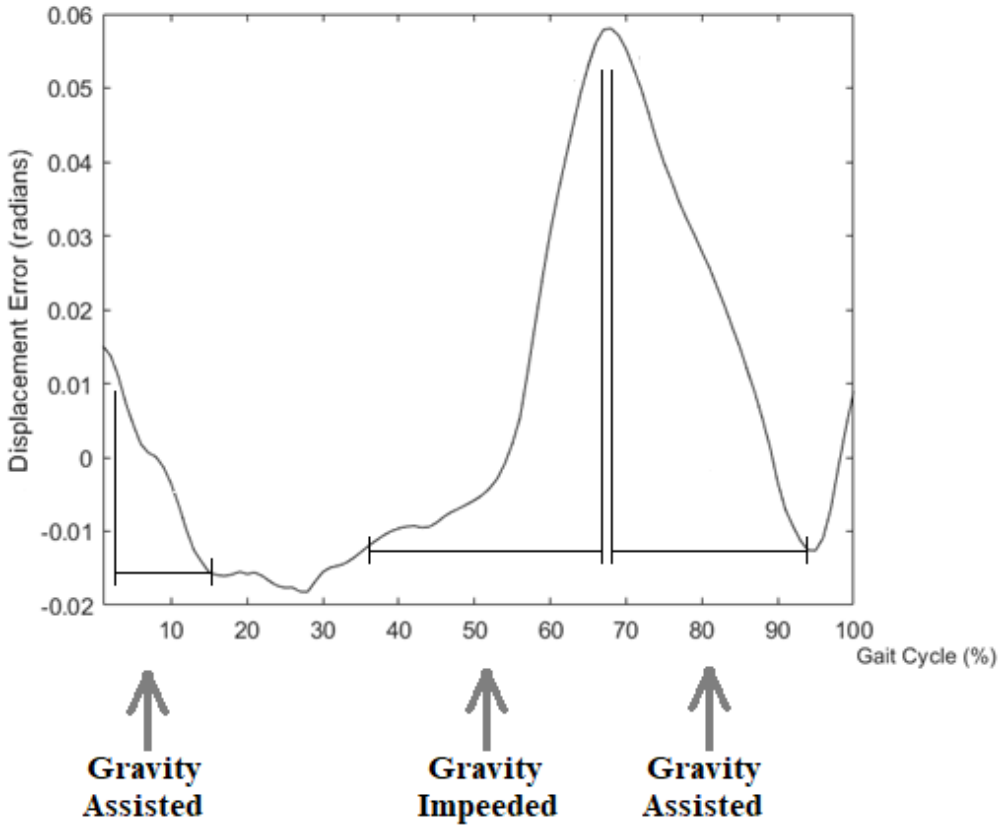

Figure 55 Gravity contribution to thigh angular position error

A similar effect is observed in the thigh motion between 50 to 90 percent gait cycle range. The error increases as the thigh is being swinged during the first half of the swing phase between the initial swing and mid-swing. During this phase the motion is impeded by gravity. As the gait cycle progresses the from mid swing to the terminal swing the error tends to reduce. During this phase the movement is assisted by gravity.

4.3.3 Control Technique

The control algorithm for the system has been kept as simple as possible and has room for improvement. The algorithm currently does not track the number of pulses generated. The system therefore relies on the update rate of the algorithm. The hardware has in-built servo tracking capability which makes the control very simple.

Currently the frequency update sequence takes place without considering the current position of the motor. The control law incorporates rate of change of position at each gate cycle to generate frequency required to manage the speed of the carriage and the thigh. However, in case of disturbances this may result in increased error in accurate trajectory tracking.

Another technique can be to update the average frequency of the gait at the mid-point between two consecutive gait cycle points. This may result in the improved accuracy and reduced lag in the system.

In the next chapter conclusion and future work is discussed.

CHAPTER 5: CONCLUSION AND FUTURE WORK

5.1 Conclusion

The control system for the transfemoral prosthesis testing platform is found to be satisfactory. The execution of the gait cycle is uniform and repeatable which is the key requirement of the cyclic testing systems. The current system does not incorporate force control or hybrid motion/ force control. The system can be run at varying gait cycle speeds for slow to normal to medium fast. It is therefore concluded that the system exhibits satisfactory capability for the control of the platform for testing transfemoral prosthesis of various types.

5.2 Future Work

The data acquisition and control system for the transfemoral prosthesis testing platform has been developed with simplest control technique in mind. This gives the system a huge room for improvements.

First and foremost, the algorithm can be further optimized to allow for the efficient execution which will improve the response of the system in real time. Lag in trajectory following can be reduced in this manner. Frequency control can be made adaptive to current position and velocity state of the system which can allow for reducing the current tracking errors.

In robotics hybrid force and motion control is a very important field of study since the forces involved in collaborative interaction between humans and robots must be kept with in range to avoid accidents. The system can be improved by implementation of force control to simulate the actual vertical ground reaction forces involved in the pedal locomotion.

The platform can be used for study in biomechanics which is a very interesting area of research. Study of neural network for motion control of the platform can be carried out and new ways of mimicking biomechanical properties of living organisms can be tested.

References

[1] A. Rad, "Human anatomy," Kenhub, [Online]. Available: https://www.kenhub.com/en/library/education/the-human-anatomy. [Accessed 07 2021].

[2] R. Whitwam, "Human Anatomy and Physiology Lab (BSB 141); Module 7: The Appendicular Skeleton," Mississippi University for Women, [Online]. Available: https://courses.lumenlearning.com/ap1x94x1/chapter/the-lower-limbs/. [Accessed 07 2021].

[3] M. Keith Bridwell, "Anatomical Planes of the Body," Remedy Health Media, LLC , [Online]. Available: https://www.spineuniverse.com/anatomy/anatomical-planes-body.

[4] J. Perry and B. . M. Judith, "Gait Analysis: Normal and Pathological Function," p. 551.

[5] Teckscan, "The Gait Cycle: Phases, Parameters to Evaluate & Technology," Tekscan, Inc., [Online]. Available: https://www.tekscan.com/blog/medical/gait-cycle-phases-parameters-evaluate-technology. [Accessed 04 2021].

[6] A. J. v. d. Bogert, T. Geijtenbeek, O. Even-Zohar, F. Steenbrink and E. C. Hardin, "A real-time system for biomechanical analysis of human movement and muscle function," *Medical & Biological Engineering & Computing* , vol. 51, p. 1069–1077, 2013.

[7] H. Miki, T. Kyo, Y. Kuroda, I. Nakahara and N. Nobuhiko Sugano, "Risk of edge-loading and prosthesis impingement due to posterior pelvic tilting after total hip arthroplasty," *Clinical Biomechanics,* vol. 29, no. 6, pp. 607-613, 2014.

[8] J. K. Moore, S. K. Hnat and A. J. Van Den Bogert, "An elaborate data set on human gait and the effect of mechanical perturbations," *PeerJ,* 2015.

[9] Nova Scotia Rehabilitation Centre, "Lower Limb Amputations Categories," Nova Scotia Rehabilitation Centre, [Online]. Available: http://www.cdha.nshealth.ca/amputee-rehabilitation-musculoskeletal-program/coping-your-amputation/lower-limb-amputations-categor. [Accessed 6 2021].

[10] Ottobock, "Above-knee waterproof prosthesis," Ottobock, [Online]. Available: https://www.ottobockus.com/products/aqualine-waterproof-above-knee-system/. [Accessed 6 2021].

[11] L. Flynn, J. Geeroms, R. Jimenez-Fabian, S. Heinz, B. Vanderborght, M. Munih, M. R. Lova, N. Vitiello and D. Lefeber, "The Challenges and Achievements of Experimental Implementation of an Active Transfemoral Prosthesis Based on Biological Quasi-stiffness: the CYBERLEGs beta-prosthesis," *Frontiers in Neurorobotics,* vol. 12, 2018.

[12] H. Giberti, F. Resta, E. Sabbioni, L. Vergani, C. Colombo, G. Verni and E. Boccafogli, "Development of a Bench for Testing Leg Prosthetics," *Special Topics in Structural Dynamics,* vol. 6, pp. 35-45, 2013.

[13] N. Petrone , G. Costa , G. Foscan, F. Bettella , G. Migliore and A. . G. Cutti , "Conceptual Design of a New Multi-Component Test Bench for the Dynamic Characterization of Running Specific Prosthesis," in *13th Conference of the International Sports Engineering Association*, Online, 2020.

[14] T. Agarwal, "A Glance on Industrial Control Systems with Control Strategies," Edgefx Technologies Pvt Ltd, [Online]. Available: https://www.efxkits.us/industrial-control-systems-and-control-strategies/. [Accessed 2021].

[15] T. ŽILIĆ, J. KASAĆ, M. ESSERT, B. NOVAKOVIĆ and Ž. ŠITUM, "Performance Comparison of Different Control Algorithms for Robot Manipulators," *Hrčak - Portal of scientific journals of Croatia,* pp. 399-407, 2012.

[16] A. J. Moshayedi, R. A. Shuvam and L. Li, "PID Tuning Method on AGV (automated guided vehicle) Industrial Robot," *Journal of Simulation and Analysis of Novel Technologies in Mechanical Engineering (JSME),* vol. 12, no. 4, pp. 53-66, 2020.

[17] A. Urquizo, "PID controller," Wikipedia, [Online]. Available: https://en.wikipedia.org/wiki/PID_controller. [Accessed 05 2021].

[18] J. Iqbal, M. Ullah, S. G. Khan, B. Khelifa and S. Cukovic, "Nonlinear control systems – A brief overview of historical and recent advances," *NonLinear Engineering,* p. 12, 2017.

[19] Q. Zhang, X. Sun, F. Tong and H. Chen, "A Review of Intelligent Control Algorithms Applied to Robot Motion Control," in *8th Annual International Conference on CYBER Technology in Automation, Control, and Intelligent Systems*, Tianjin, China, 2018.

[20] B. Zhang, W. Wei , Y. Ju, J. Lin, Z. Gao and Y. Zhong, "Design of servo motor synchronous control system for instrumented wheelset calibration test bench," in *29th Chinese Control And Decision Conference (CCDC)*, Chongqing, China, 2017.

[21] L. Wang and C. Zhong, "Trajectory Tracking of Robot Based on Fractional Order Fuzzy PI Controller," in *International Conference on Sensing,Diagnostics, Prognostics, and Control (SDPC)*, Xi'an, China, 2018.

[22] J. Ye and X. Gao, "Application Research of Servo Circuit Based on PLC and Configuration Software," in *12th International Symposium on Computational Intelligence and Design (ISCID)*, 2019.

[23] H. M. Saputra, A. Nurhakim and M. N. Firdaus, "Servo Motor Controller Device for Stewart Platform Based on Simple Pulse Generator," in *International Conference on Radar, Antenna, Microwave, Electronics, and Telecommunications (ICRAMET)*, Tangerang, Indonesia, 2019.

[24] Q. Ai, Q. Yang, M. Li, X. Feng and W. Meng, "Implementing Multi-DOF Trajectory Tracking Control System for Robotic Arm," in *10th International Conference on Measuring Technology and Mechatronics Automation (ICMTMA)*, Changsha, China, 2018.

[25] M. Idres, O. Mustapha and M. Okasha, "Quadrotor trajectory tracking using PID cascade control," in *IOP Conference Series: Materials Science and Engineering*, Putrajaya, Malaysia, 2017.

[26] H. Richter, D. Simon, W. A. Smith and S. Samorezov, "Dynamic modeling, parameter estimation and control of a leg prosthesis test robot," *Applied Mathematical Modelling,* vol. 39, no. 2, pp. 559-573, 2015.

[27] M. Galicki, "Trajectory tracking control of a mobile manipulator with an external force compensation," *Bulletin Of The Polish Academy Of Sciences: Technical Sciences,* p. 11, 2021.

[28] H. Hu, S. Xiao and H. Shen, "Modified Linear Active Disturbance Rejection Control for Uncertain Robot Manipulator Trajectory Tracking," *Mathematical Problems in Engineering,* vol. 2021, p. 13, 2021.

Appendix

Table 1 STM32F407 Discovery Pin Connections

Pin Number LQFP100	Pin Name (function after reset)	Pin Type	Alternate Function(s)	Label
6	VBAT	Power		
10	VSS	Power		
11	VDD	Power		
12	PH0-OSC_IN	I/O	RCC_OSC_IN	
13	PH1-OSC_OUT	I/O	RCC_OSC_OUT	
14	NRST	Reset		
19	VDD	Power		
20	VSSA	Power		
21	VREF+	Power		
22	VDDA	Power		
23	PA0-WKUP	I/O	TIM5_CH1	Thigh Motor Encoder Channel A
24	PA1	I/O	TIM5_CH2	Thigh Motor Encoder Channel B
25	PA2	I/O	USART2_TX	PC Serial Connection
26	PA3	I/O	USART2_RX	PC Serial Connection
27	VSS	Power		
28	VDD	Power		
30	PA5	I/O	TIM2_CH1	Hip Motor Encoder Channel A
40	PE9	I/O	TIM1_CH1	Hip Motor Drive Forward Pulse Train
42	PE11	I/O	TIM1_CH2	Hip Motor Drive Reverse Pulse Train
49	VCAP_1	Power		
50	VDD	Power		
59	PD12	I/O	TIM4_CH1	Thigh Motor Drive Forward Pulse Train
60	PD13	I/O	TIM4_CH2	Thigh Motor Drive Reverse Pulse Train
72	PA13	I/O	SYS_JTMS-SWDIO	
73	VCAP_2	Power		
74	VSS	Power		
75	VDD	Power		
76	PA14	I/O	SYS_JTCK-SWCLK	
89	PB3	I/O	TIM2_CH2	Hip Motor Encoder Channel B

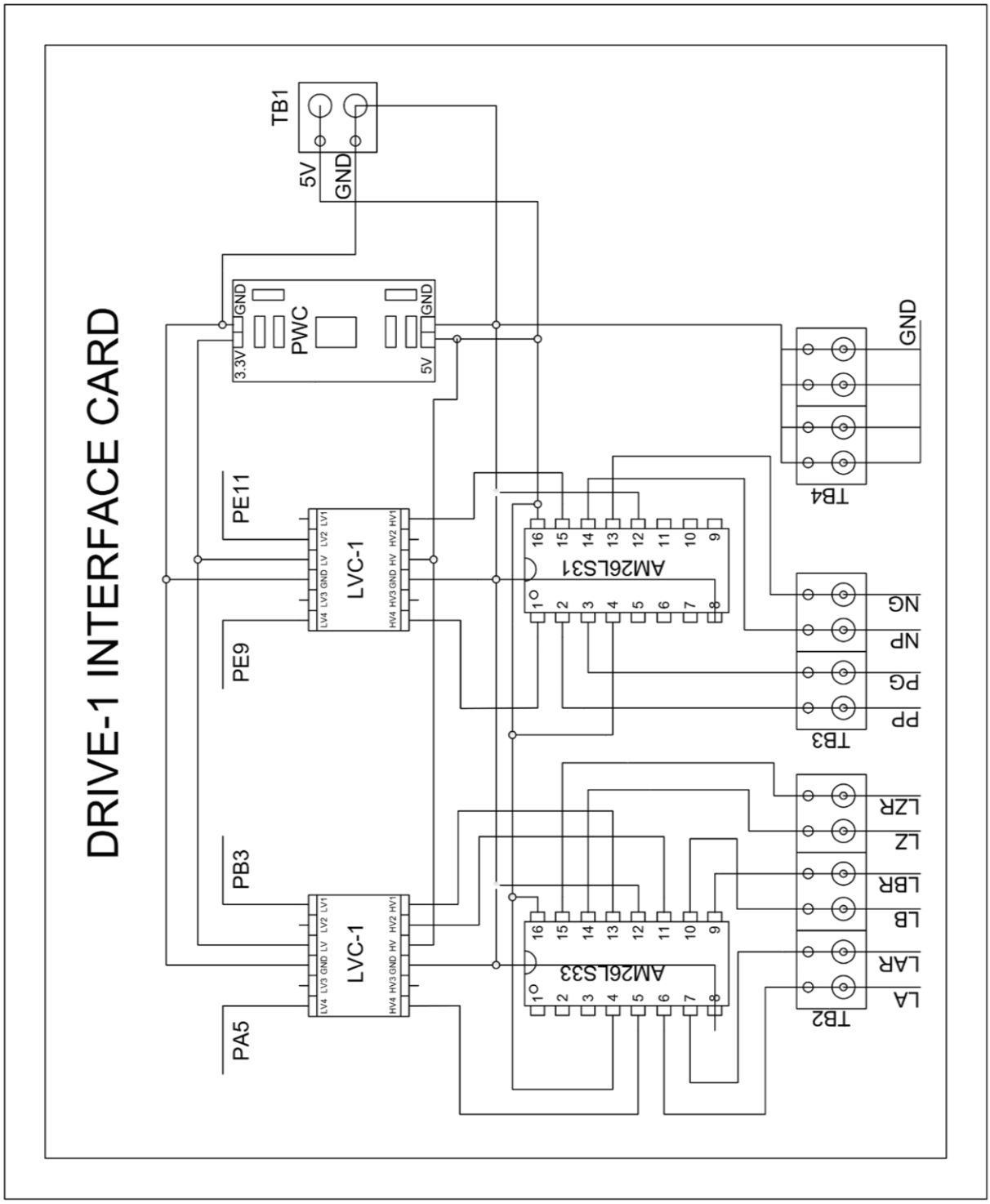

Figure 56 Interface Card Schematic for Hip Motion Drive

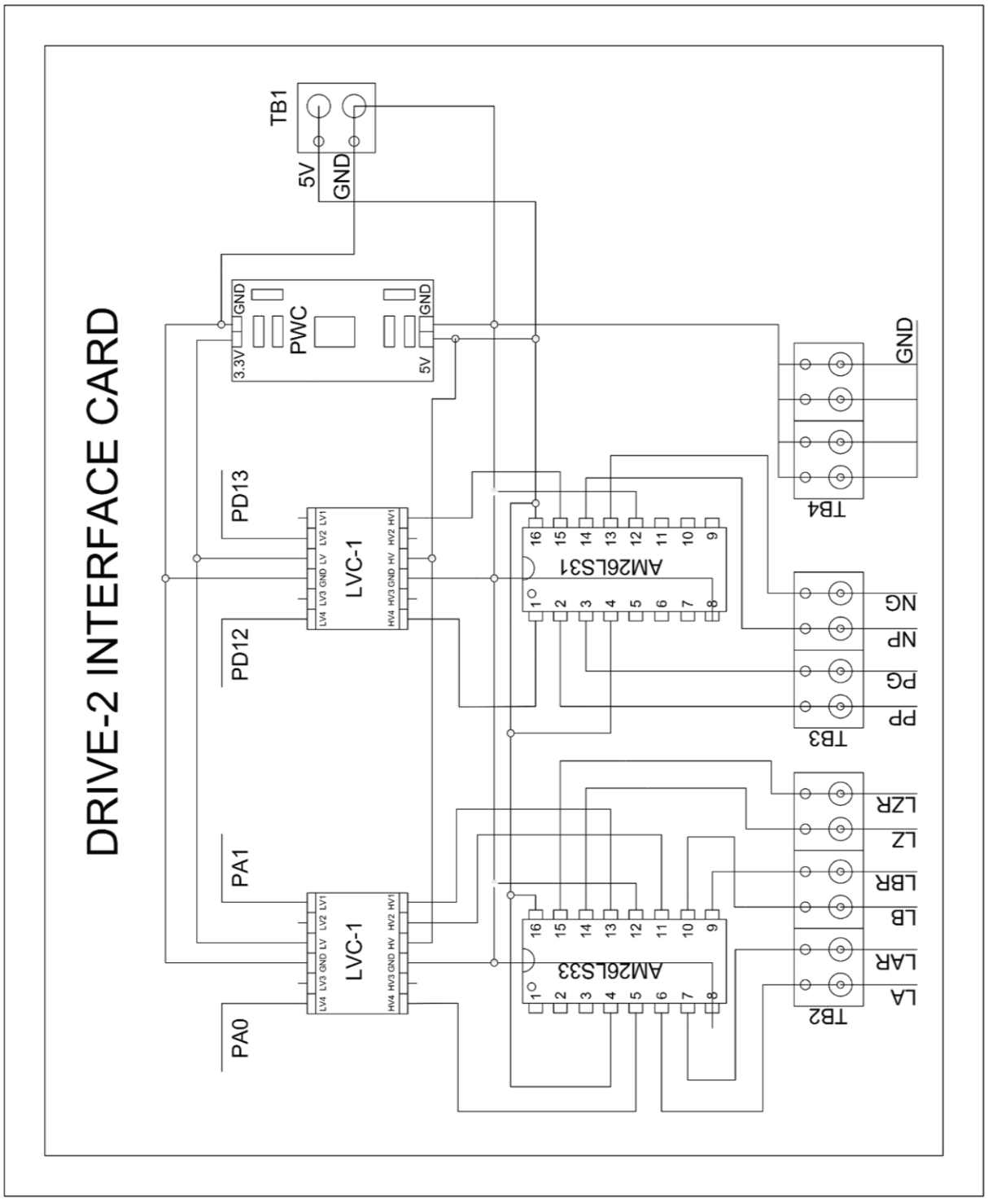

Figure 57 Interface Card Schematic for Thigh Motion Drive

Completion Certificate

It is certified that the thesis titled **"Development of Data Acquisition and Control System for Transfemoral Prosthesis Testing Platform"** submitted by Registration No. 00000205287, NS Afnan Ahmed Yaqub of MS-17 Mechatronics Engineering is completed in all respects as per the requirements of Main Office, NUST (Exam branch).

Supervisor: _____

Dr. Mohsin Islam Tiwana

Date: _____ Aug, 2021